ARTICLE IN PRESS

Palaeogeography, Palaeoclimatology, Palaeoecology xxx (xxxx) xxx-xxx

FISEVIER

Contents lists available at ScienceDirect

Palaeogeography, Palaeoclimatology, Palaeoecology

journal homepage: www.elsevier.com/locate/palaeo



Origin of paleovalleys on the Rio Grande do Sul Shield (Brazil): Implications for the extent of late Paleozoic glaciation in west-central Gondwana

Nicholas D. Fedorchuk^{a,*}, John L. Isbell^a, Neil P. Griffis^b, Isabel P. Montañez^b, Fernando F. Vesely^c, Roberto Iannuzzi^d, Roland Mundil^e, Qing-Zhu Yin^b, Kathryn N. Pauls^a, Eduardo L.M. Rosa^c

- ^a Department of Geosciences, University of Wisconsin-Milwaukee, Milwaukee, WI 53211, USA
- ^b Department of Earth and Planetary Sciences, University of California, Davis, Davis, CA 95616, USA
- ^c Department de Geologia, Universidade Federal do Paraná, Curitiba, PR, Caixa Postal 19001, CEP 81531-980, Brazil
- d Centro de Investigações do Gondwana, Instituto de Geociências, Universidade Federal do Rio Grande do Sul, Porto Alegre, RS 91.509-900, Brazil
- ^e Berkeley Geochronology Center, Berkeley, CA 94709, USA

ARTICLE INFO

Keywords: Late Paleozoic ice age Paraná Basin Detrital zircon geochronology Itararé Group Rio Bonito Formation Pull-apart basin

ABSTRACT

The location, longevity, and geographic extent of late Paleozoic ice centers in west-central Gondwana remain ambiguous. Paleovalleys on the Rio Grande do Sul Shield of southernmost Brazil have previously been interpreted as fjords carved by outlet glaciers that originated in Africa and emptied into the Paraná Basin (Brazil). In this study, the sedimentology, stratigraphy, and provenance of sediments infilling two such paleovalleys (the Mariana Pimentel and Leão paleovalleys) were examined in order to test the hypothesis that an ice center over present day Namibia drained across southernmost Brazil during the Carboniferous and Permian. Contrary to previous findings, the facies assemblage from within the paleovalleys is inconsistent with a fjord setting and no clear evidence for glaciation was observed. The facies show a transition from a non-glacial lacustrine/estuarine environment, to a fluvial-dominated setting, and finally to a restricted marine/estuarine environment. Detrital zircon results present a single population of Neoproterozoic ages (c. 800-550 Ma) from the paleovalley fill that matches the ages of underlying igneous and metamorphic basement (Dom Feliciano Belt) and is incongruent with African sources that contain abundant older (Mesoproterozoic, Paleoproterozoic, and Archean) zircons. Furthermore, results suggest that the formation of the paleovalleys and the deposition of their fill were controlled by the reactivation of Neoproterozoic basement structures during the Carboniferous and Permian. The lack of evidence for glaciation in these paleovalleys highlights the need for detailed studies of supposed late Paleozoic glacial deposits. These results are supportive of the hypothesis that well-established glacial sediments on the Rio Grande do Sul Shield (southern margin of the Paraná Basin) may be the product of a separate lobe extending north across Uruguay, rather than a single, massive ice sheet draining west from Africa.

1. Introduction

Earth's deep-time climate alternates between long duration (100s of Myr) greenhouse/hothouse and shorter duration (10s Myr to 100 Myr) icehouse conditions. Of the three major Phanerozoic icehouse intervals, the Late Paleozoic Ice Age (LPIA), which extended for ~113 Myr from the Late Devonian (Famennian) until the Late Permian (Wuchiapingian), was the most spatially and temporally extensive (e.g. Fielding et al., 2008b; Frank et al., 2015; Isbell et al., 2003, 2012; Montañez and Poulsen, 2013). The study of this penultimate icehouse event is essential to understanding deep-time climate change and ice ages' influence on Earth systems (e.g. Gastaldo et al., 1996; Horton

et al., 2010; Montañez and Soreghan, 2006; Montañez et al., 2011). An important aspect of determining the mechanistic relationship between ice extent and global climate is identifying the timing and extent of ice centers during glacial intervals. However, the nature of ice volume fluctuations during the LPIA in time and space remain enigmatic (Buggisch et al., 2011; Chen et al., 2013, 2016; Fielding et al., 2008a, b; Frank et al., 2015; Isbell et al., 2003, 2012; Montañez and Poulsen, 2013; Rygel et al., 2008; Veevers and Powell, 1987; Ziegler et al., 1997). Recent studies of mid-to-high-latitude glaciogenic deposits suggest that the LPIA consisted of multiple ice centers and shorter (> 10 Myr) glacial intervals separated by warm intervals of similar duration (e.g. Fielding et al., 2008a, b; Gulbranson et al., 2010;

E-mail address: fedorch2@uwm.edu (N.D. Fedorchuk).

https://doi.org/10.1016/j.palaeo.2018.04.013

Received 3 December 2017; Received in revised form 16 March 2018; Accepted 17 April 2018 0031-0182/ © 2018 Elsevier B.V. All rights reserved.

^{*} Corresponding author.

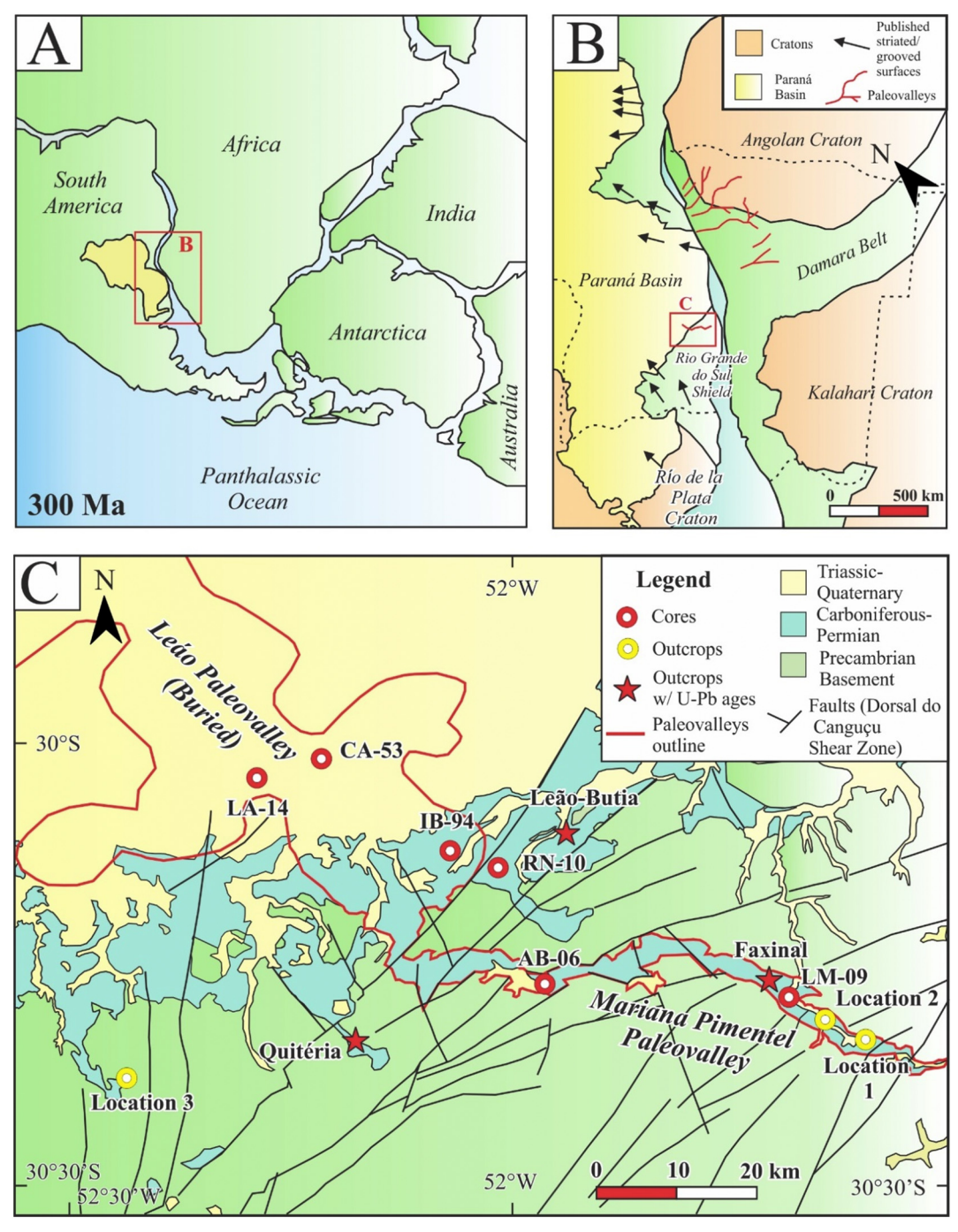
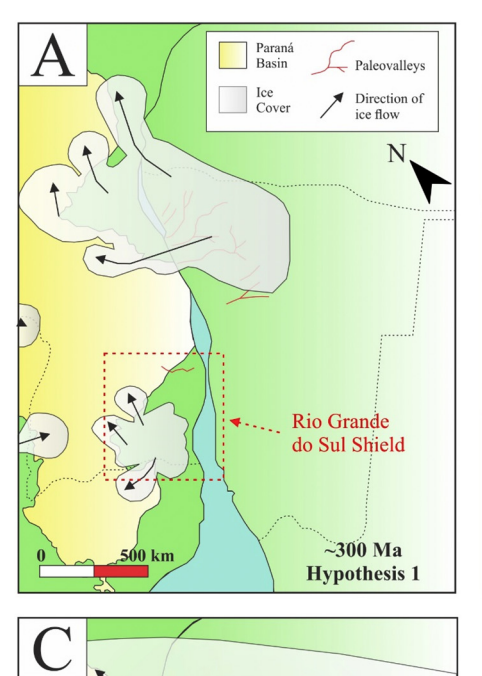


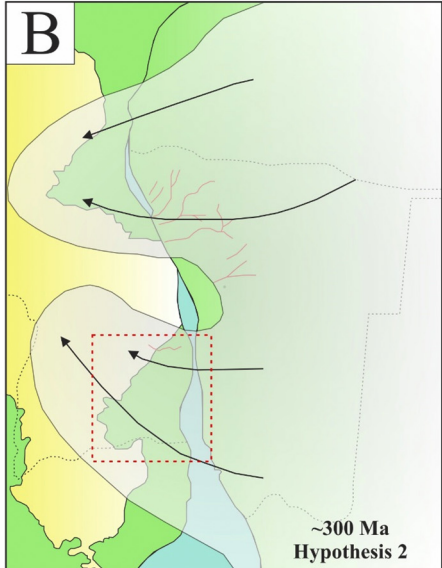
Fig. 1. Paleogeography and study location. A. Gondwana paleogeography and Paraná Basin (yellow) during Pennsylvanian (after PLATES/UTIG; Fallgatter and Paim, 2017). B. Southern and eastern margin of Paraná Basin relative to western Africa. Paleovalleys indicated by red lines. Published striated/grooved surface locations with interpreted ice flow directions represented by black arrows (after Fallgatter and Paim, 2017; Rosa et al., 2016). C Study location with Mariana Pimentel and Leão paleovalleys outlined in red. Outcrops indicated by orange/white circles and cores indicated by red/white circles (after Lopes, 1995; Tedesco et al., 2016). Location 1 at 30°18′27.78″S, 51°38′35.22″W, Location 2 at 30°19′40.91″S, 51°35′47.15″W, Location 3 at 30°22′66″S, 52°25′33.13″W. (For interpretation of the references to colour in this figure legend, the reader is referred to the web version of this article.)

Iannuzzi and Pfefferkorn, 2002; Isbell et al., 2003, 2012; López-Gamundí, 1997; Montañez and Poulsen, 2013; Visser, 1997). However, to fully understand the complexity of the glaciation, each ice center and its associated depositional basin(s) needs to be thoroughly examined.

The Paraná Basin of southern Brazil, Uruguay, Paraguay, and northeastern Argentina contains a largely complete, mid-latitude (~45–55°S) record of LPIA glaciation (Fig. 1A) (e.g. Milani et al., 1998; Rocha-Campos et al., 2008; Torsvik and Cocks, 2013; Vesely et al., 2015). Temperate ice sheets at such paleolatitudes would have been

sensitive to climate variability, making this basin a key to reconstructing the stability of ice centers. In particular, the location, extent, dynamics, and timing of glaciation on the southernmost margin of the Paraná Basin remain poorly understood despite numerous studies of Carboniferous-Permian deposits in this region (e.g. Guerra-Sommer et al., 2008a, b, c; Holz, 1999; Holz, 2003; Ribeiro et al., 1987; Rocha-Campos et al., 2008; Tedesco et al., 2016; Tomazelli and Soliani Júnior, 1982; Tomazelli and Soliani Júnior, 1997). This area is underlain by an assemblage of mostly Neoproterozoic igneous and metamorphic





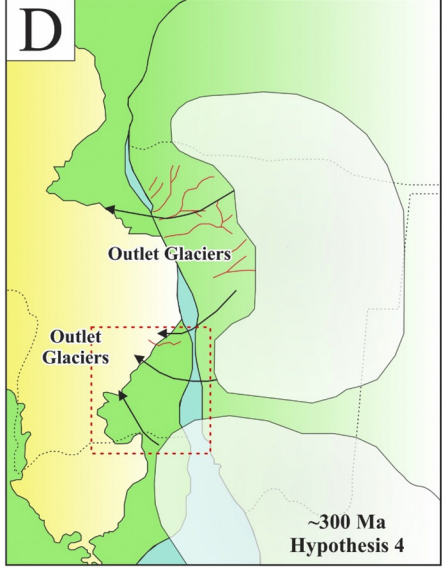


Fig. 2. Hypotheses for size and location of glaciers entering Paraná Basin during late Carboniferous. Rio Grande do Sul Shield in red box. A. Hypothesis 1: multiple small ice centers on paleotopographic highs around basin margins (after Rocha-Campos et al., 2008; Santos et al., 1996). B. Hypothesis 2: single massive ice sheet from Africa or Antarctica (after Visser, 1993). C. Hypothesis 3: two separate, unconfined lobes entering basin, one extending north from Uruguay and another extending west from Namibia (after Crowell and Frakes, 1975; Frakes and Crowell, 1972). D. Hypothesis 4: outlet glaciers entering southern and eastern margin of basin though paleovalleys originating in Africa (after Fallgatter and Paim, 2017; Tedesco et al., 2016). (For interpretation of the references to colour in this figure legend, the reader is referred to the web version of this article.)

terranes known as the Rio Grande do Sul Shield (RGS) (e.g. Gray et al., 2008; Oyhantçabal et al., 2011) that has been interpreted by some authors as the crustal root of a topographic high during the late Paleozoic (Fig. 1B) (e.g. Rocha-Campos et al., 2008; Santos et al., 1996). Diamictites, lonestone-bearing rhythmites, striated clasts, faceted clasts, and grooved surfaces have all been described from late Paleozoic units on the RGS, suggesting that at least part of this area was glaciated (e.g. Corrêa da Silva, 1978; Delaney, 1964; Santos et al., 1996; Tomazelli and Soliani Júnior, 1982; Tomazelli and Soliani Júnior, 1997).

~300 Ma Hypothesis 3

There are competing hypotheses for the occurrence and extent of glaciation that influenced the southern portion of the Paraná Basin during the LPIA. These hypotheses range from alpine glaciation, ice caps ($<5\times10^4~\rm km^2$), small ice sheets ($5\times10^4~\rm to~1\times10^6~\rm km^2$), to massive ice sheets ($1\times10^6~\rm to~35\times10^6~\rm km^2$) (Fig. 2). Such size variations represent vastly different ice volumes and imply that either ice was only locally present, centered locally on the RGS, centered in Africa, or extended to the Paraná Basin from Antarctica (e.g. Crowell and Frakes, 1975; Crowell, 1999; Frakes and Crowell, 1972; Rocha-Campos et al., 2008; Santos et al., 1996; Visser, 1993). How ice entered the basin (as alpine glaciers, outlet glaciers draining through paleovalleys, or as unconfined lobes) and its extent (confined to basin

margins vs. extending across the basin) is also in dispute (Fig. 2) (e.g. Fallgatter and Paim, 2017; Gesicki et al., 1998; Gesicki et al., 2002; Holz et al., 2008; Riccomini and Velázquez, 1999; Rocha-Campos et al., 2008; Santos et al., 1996; Tedesco et al., 2016). Determining these details is fundamental to understanding the nature of glaciation in the Paraná Basin and its global impact during the LPIA.

The Mariana Pimentel and Leão paleovalleys (Fig. 1C), located on the NE of the RGS, are critical in resolving the volume of ice that entered the southern Paraná Basin (e.g. Fallgatter and Paim, 2017; Guerra-Sommer et al., 2008b; Iannuzzi et al., 2006; Iannuzzi et al., 2010; Lopes, 1995; Paim et al., 1983; Silveira, 2000; Tedesco et al., 2016; Visser, 1987). These two paleovalleys, often considered as a single paleovalley system, are interpreted by some authors as glacial fjords (e.g. Tedesco et al., 2016). These paleovalleys are also viewed by some as directly linked to glacial paleovalleys in the Windhoek Highlands that drained ice westward out of Namibia and into eastern South America (e.g. Fallgatter and Paim, 2017; Martin, 1981; Tedesco et al., 2016). Identification of the depositional history and sediment provenance of strata in these paleovalleys will help define the extent of glaciation in the Paraná Basin and test whether the Mariana Pimentel and Leão paleovalleys were fjords with either locally sourced glacial flow, glacial flow originating from the Windhoek Highlands, or glacial

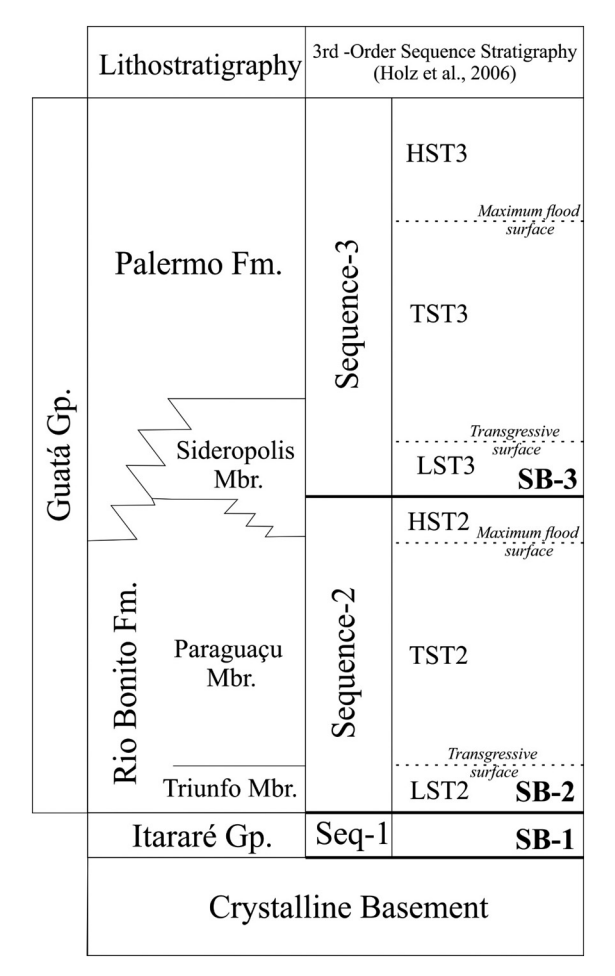


Fig. 3. Third-order sequence stratigraphic framework for southern and eastern Paraná Basin (after Holz et al., 2006). SB = sequence boundary, LST = low-stand systems tract, TST = transgressive systems tract, HST = highstand systems tract.

flow from farther afield in Africa/Antarctica.

2. Geologic setting

The Paraná Basin is an intracratonic basin located in Brazil, Paraguay, Uruguay, and Argentina that formed following the Brasiliano orogeny (Late Proterozoic–early Paleozoic). Carboniferous and Permian lithostratigraphic units on the southern margin of the Paraná Basin and described from the paleovalleys are the Itararé Gp. and the Guatá Gp., (Fig. 3) (e.g. Holz, 1999, 2003). On the RGS, these units rest nonconformably on Precambrian basement.

The Itararé Gp. contains the glaciogenic sediments found throughout the Paraná Basin and is described in the subsurface throughout the Paraná Basin as consisting of three formations. These are (from oldest to youngest) the Lagoa Azul Fm., the Campo Mourão Fm., and the Taciba Fm. (e.g. França and Potter, 1991). However, only the youngest Taciba Fm. occurs in the southernmost part of the basin, which is the focus of this study (e.g. Holz et al., 2010).

Palynological studies suggest that the Itararé Gp. was deposited during the Pennsylvanian and, in some areas, extends into the Early Permian (Cisuralian) (e.g. Souza, 2006). Numerous attempts to radiometrically date ash beds in the overlying Rio Bonito Fm. have produced a wide range of ages for the contact between the Itararé Gp. and the Rio Bonito Fm on the RGS (e.g. Cagliari et al., 2016; Guerra-Sommer et al., 2008a, b, c; Matos et al., 2001; Mori et al., 2012; Simas et al., 2012). A recent re-analysis by Griffis et al. (2018) of several ash beds contained within coal seams (tonsteins) using chemical abrasion thermal ionizing

mass spectrometry (CA-TIMS) U-Pb geochronology more precisely constrains the findings of Cagliari et al. (2016) that suggest glaciation on the southernmost margin of the basin may have been entirely Carboniferous, with the earliest post-glacial coal beds occurring around the Gzhelian/Asselian boundary at \sim 298–297 Ma.

The Rio Bonito and the Palermo Fms, of the Guatá Gp, overlie the Itararé Gp. The Rio Bonito Fm. is interpreted to rest unconformably on the Itararé Gp strata in the southern part of the Paraná Basin (Fig. 3) (e.g. Holz et al., 2006) and is distinguished as being the fluvio-deltaic coal-forming interval. However, alluvial fan, fluvial, lagoonal, and deltaic sediments are all contained in the Rio Bonito Fm. In some areas. the Palermo Fm. conformably overlies and interfingers with the Rio Bonito Fm., representing the offshore transition/lower shoreface facies that are in part time-equivalent to the Rio Bonito Fm. (Fig. 3) (e.g. Holz, 2003; Holz et al., 2006). In other areas, an angular unconformity exists between the Rio Bonito and Palermo Fms., which has been used to suggest active tectonism on the RGS during the Early Permian (Holz et al., 2006). The Palermo Fm. consists of laminated and bioturbated sandstones, siltstones, and mudstones (Holz, 1999, 2003). Taken together, the Rio Bonito and the Palermo fms. are part of a 2nd order transgressive systems tract (Holz, 2003; Holz et al., 2006).

3. Location: Mariana Pimentel and Leao paleovalleys

The Mariana Pimentel Paleovalley is a narrow, trough-shaped (\sim 0.5–6.5 km wide and > 80 km long) feature cut into Neoproterozoic igneous and metamorphic basement of the Dom Feliciano Belt (Fig. 1C). The borders of the paleovalley have been noted to correspond closely with faults of the Neoproterozoic Dorsal do Canguçu Shear Zone (Fig. 1C) (e.g. Guerra-Sommer et al., 2008b; Ribeiro et al., 1987). The best-exposed outcrop (Location 1) from the Mariana Pimentel Paleovalley is a ~50 m thick section located in an abandoned kaolinite quarry called Morro Do Papaléo, located ~7 km NW of the town of Mariana Pimentel (Fig. 1C). Location 2 is a ~8 m thick section from a roadside quarry that shows the base of the section and the contact with crystalline basement. It is located ~3 km northwest of Mariana Pimentel. A third outcrop used in this study (Location 3) is a road cut located \sim 45 km outside of the paleovalley (Fig. 1C). This \sim 7.5 m thick section shows the nonconformity between granite basement and the post-glacial Rio Bonito Fm.

The Mariana Pimentel Paleovalley is connected to a wider and shorter (~15 km wide and ~55 km in length) paleotopographic depression near Minas do Leão, which has been named the Leão Paleovalley (Fig. 1C). The Leão Paleovalley is only observed in the subsurface through core descriptions and geophysical logs that show basement relief (Lopes, 1995). This wider paleo-depression extends north into the Paraná Basin. Despite their description as two separate paleovalleys (e.g. Tedesco et al., 2016), some authors refer to them as the Leão-Mariana Pimentel Paleovalley (e.g. Lopes, 1995; Ribeiro et al., 1987) and suggest that they were part of the same ancient drainage system.

Tonsteins from the paleovalleys were originally thought to be coeval to tonstein-bearing coals located across the RGS that are stratigraphically near the base of the Rio Bonito Fm. (e.g. Guerra-Sommer et al., 2008c). However, two tonsteins within and just outside the paleovalleys (Fig. 1C) were found to have U-Pb ages of ~285 Ma (Faxinal location; Griffis et al., 2018) and ~289 Ma (Leão-Butia location; Simas et al., 2012), which are respectively 12 and 8 Myr younger than tonsteins from the base of the Rio Bonito (~297 Ma; Quitéria outcrop) (e.g. Griffis et al., 2018). This makes it clear that there are separate coalforming intervals in the southernmost Paraná Basin. Coals from within the paleovalleys are younger than those located on paleotopographic highs < 10 km outside the paleovalleys (Quitéria outcrop; Fig. 1C). Notably, older coals, equivalent to the Quitéria outcrop, are not found within the paleovalley fill (e.g. Griffis et al., 2018).

4. Methods

4.1. Facies analysis

Stratigraphic sections were measured and outcrops were photographed in the field at Location 1 (Morro do Papaléo), Location 2, and Location 3 (outside of paleovalleys). Observations were made of grain size, lithology, sorting, sedimentary structures, paleocurrent orientations, nature of contacts, sediment body geometries, unit thicknesses, and relationships with adjacent strata. Additionally, 6 cores (LM-09, AB-06, RN-10, IB-94, CA-53, and LA-14) were measured, described, and photographed. Core RN-10 is from outside of the paleovalleys. Cores used in this study are housed at the Companhia de Pesquia de Recursos Minerais (CPRM) facility in Caçapava do Sul and on the campus of Universidade do Vale do Rio do Sinos (UNISINOS), located in São Leopoldo.

4.2. Detrital zircon U-Pb geochronology

Two detrital zircon samples were analyzed for this study. One sample (MDP6) was collected from a medium quartz sandstone, previously described as lowermost Rio Bonito Fm. (e.g. Iannuzzi et al., 2006; Smaniotto et al., 2006) at the Location 1 outcrop. A second sample (MP) was collected at Location 2 from a medium pebbly quartz sandstone previously described as Itararé Gp. (e.g. Iannuzzi et al., 2006; Smaniotto et al., 2006). This sample was collected at the base of the section, ~0.5 m above granite basement. Sediment provenance was assessed using detrital zircon (U-Pb) geochronology in order to determine if there was local versus extra-basinal sources. Laser ablation inductively coupled plasma mass spectrometry (LA-ICP-MS) analyses were conducted at the University of California, Davis. Kernel density estimate plots were created on the provenance package for R and DensityPlotter with an adaptive bandwidth (Vermeesch, 2012; Vermeesch et al., 2016). Complete detrital zircon data and a detailed description of laser ablation methods can be found in the supplemental data files.

5. Results

5.1. Facies analysis and process interpretations

The sedimentary fill of the Mariana Pimentel and Leão paleovalleys can be divided into seven distinct facies which are observed in the cores and outcrops: a sandy conglomerate and breccia facies, a rhythmite facies, a mudrock/fine-grained sandstone facies, a cross-stratified sandstone facies, a diamictite facies, a root-trace-bearing mudrock facies, and a heterolithic bioturbated facies (Table 1). These facies are described here as occurring in either the lower, middle, and/or upper section of the paleovalley fill which are later correlated to facies associations. Classification of poorly sorted sediments is based on Hambrey and Glasser (2003). Facies codification is adapted from Farrell et al. (2012) and Benn and Evans (2010).

5.1.1. Sandy conglomerate and breccia facies (Gm/Gp)

The sandy conglomerate and breccia facies (Gm/Gp) consists of sandy conglomerate, breccia, pebbly sandstone, and diamictite beds that occur in the lower and middle portions of the paleovalley fill (Location 2; cores LA-14, CA-53, IB-94, RN-10, and LM-09). This facies often rests directly on igneous and metamorphic basement rocks where it contains a weathering profile that grades upward over 1–2 m from unweathered basement, to basement with chemically altered feldspar phenocrysts, to brecciated basement rocks, to completely disaggregated sandy diamictite or breccia, and ends in conglomerate composed entirely of basement rocks (Fig. 4A) (e.g. Location 2; cores LM-09, RN-10, IB-94, and LA-14). Elsewhere in the succession, this facies is 10 cm to 3 m thick and consists of massive (Gm) and planar cross-bedded (Gp) sandy conglomerate. Interbeds of clast-poor to clast-rich, massive and

stratified, sandy diamictite, mudstone with root traces and coalified organic matter, and pebbly sandstone are also found in this facies. Clasts are angular to rounded and range from granule to cobble sized. Clasts are composed of granite, gneiss, k-feldspar, and quartz, which closely match the composition of the underlying basement rocks. No exotic clasts were found. The Gm/Gp facies is associated with the mudrock/fine-grained sandstone facies (Fl/Fm) and the rhythmite facies (Flv) in the lower portion of the paleovalley fill. It also occurs in association with the root-trace-bearing mudrock facies (Mrt), the diamictite facies (Dmm/Dms), and the cross-stratified sandstone (St/Sp) facies in the middle portion of the paleovalley fill.

The Gm/Gp facies is interpreted as humid alluvial fan and subaqueous fan delta deposits from both a marginal lacustrine/estuarine and alluvial environment. The clast composition, angular grains, and weathering profile are suggestive of in-situ weathering of basement with minimal erosion and transport. The alteration between conglomerate and diamictite beds is consistent with the surface of a fan that experienced both episodic, turbulent sheet and debris flows during discharge events (e.g. Bull, 1977; Mack and Rasmussen, 1984; Nemec and Steel, 1984). The mudstone interbeds with root traces and coalified material are paleosols associated with subaerial exposure on the fan surface (e.g. Fielding, 1987; Ridgway and Decelles, 1993). The interpretation of some beds within the Gm/Gp facies as subaqueous fan delta deposits is based on the interfingering of rhythmite (Flv) or mudrock/ fine-grained sandstone (Fl/Fm) beds. The weathering profiles observed in both cores and in outcrop are indicative of igneous and metamorphic basement that was exposed at the surface for a long enough period of time to experience chemical weathering.

5.1.2. Rhythmite facies (Flv)

The rhythmite facies (Flv) occurs as laterally continuous packages up to 50 m thick (Location 1 and 2; cores CA-53 and AB-06). This facies is located in the lower third of the paleovalley fill and typically overlies either the conglomerate and breccia (Gm/Gp) facies or igneous/metamorphic basement (Location 2) (Fig. 4B). The Flv facies is also associated with the mudrock/fine-grained sandstone (Fl/Fm) facies (Fl/ Fm). Rhythmites consist of stacked, sharp to erosional-based (5 mm-10 cm thick) couplets composed of either fine-grained quartz sandstone or siltstone bases that grade upwards into mudstone caps (Fig. 4C). The sandstone portion of couplets contain climbing ripples (Fig. 5A), load and flame structures (Fig. 5B), and rhythmite rip-up clasts (Fig. 5C). Extremely rare lonestones (granule and pebble-sized) of k-feldspar and granite occur in this unit (only 2 pebbles were found in all of the strata examined) (Fig. 6A). In cores, discrete zones of brittle faulting (Fig. 5D) with calcite vein fill occur, as well as zones of intense ductile deformation with folded rhythmite beds (Fig. 6B). Rhythmite beds in core CA-53 also display sheared laminations and contain brecciated zones (Fig. 6C). Rhythmite couplets in core AB-06 are thickest near the base of the core and gradually thin upwards where they transition to a carbonaceous mudstone (Fl facies).

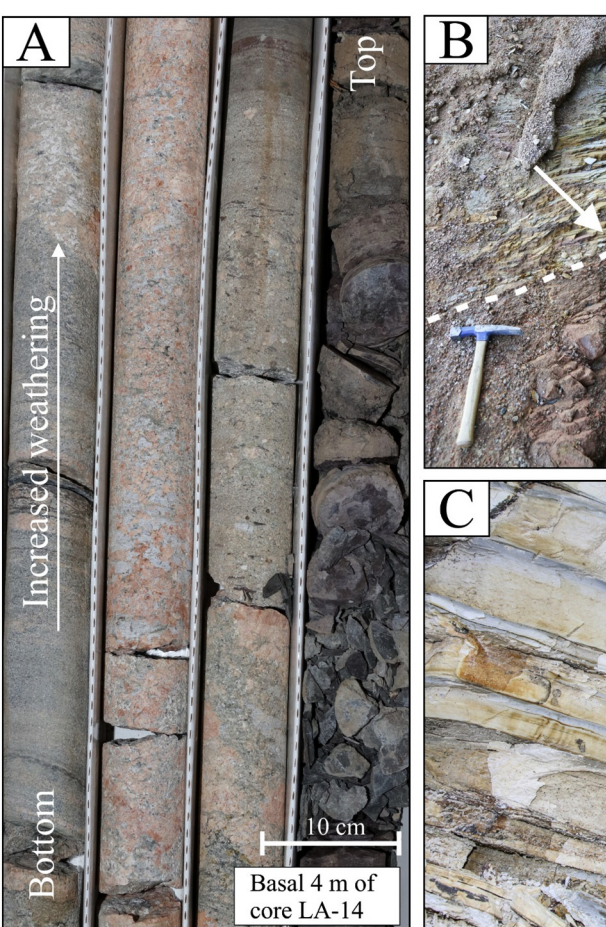
The Flv facies is interpreted as the product of dilute, surge-like turbidity currents and/or quasi-continuous hyperpycnal flows in a prodeltaic lacustrine or estuarine environment. The erosive and sharp contacts between couplets, combined with variable and large couplet thicknesses implies that each couplet was deposited during an individual, surge-like flow rather than as a long-duration suspension settling event. Climbing ripples and rip-up clasts demonstrate that erosive, tractive, underflow currents deposited the lower part of the couplet while normal grading suggest that hydraulic sorting and settling from suspension occurred following dissipation of the current. Load and flame structures indicate that an insufficient amount of time had passed between flow events to allow for compaction and water loss of previously deposited couplets. The features discussed above are typical of either surge-like turbidity currents (e.g. Talling et al., 2012) or quasi-steady hyperpycnal flows produced by increased river discharge during episodic flooding events (e.g. Crookshanks and Gilbert, 2008;

 Table 1

 Lithofacies codes, descriptions, and paleoenvironmental interpretations.

Lithofacies name	Symbol	Lithologies	Key features and sedimentary structures	Bed thickness	Interpretation
Sandy conglomerate and breccia facies	Gm (massive) Gp (planar cross beds)	Sandy conglomerate and breccia, interbeds of clast-poor to clast-rich sandy diamictite, pebbly sandstone, and mudstone	Mostly clast supported with rare matrix support, clast composition consistent with local basement material, interbeds contain coalified material and root traces	~10 cm to 3 m thick, interbeds range from ~4 cm to 0.5 m thick	Alluvial fans or subaqueous fan deltas in marginal lacustrine or estuarine setting
Rhythmite facies	Flv	Fine to very fine sandstone, siltstone, and mudstone	Normally graded sand or silt rhythmites with mudstone caps, climbing ripples, flame structures, rip-up clasts, very rare outsized clasts, zones of brittle and ductile deformation	${\sim}5\text{mm}$ to 10 cm thick couplets, up to ${\sim}50\text{m}$ thick packages of rhythmites	Distal turbidity currents or hyperpycnal flows in lacustrine or estuarine setting
Mudrock/fine-grained sandstone facies	Fl (laminated) Fm (massive)	Mudstone, siltstone, very fine to fine sandstone	Plant fossils, organic debris, laminated or massive	~3 cm to 10 m thick massive beds, ~1 m to 10 m thick packages of finely laminated sediment	Stable, low energy conditions, sediment settling out of suspension, in lacustrine or estuarine setting
Cross-stratified sandstone facies	St (trough cross beds) Sp (planar cross beds)	Very fine to very coarse quartz sandstone, sometimes pebbly	Planar and trough cross beds, normally graded, sometimes contains granule to pebble sized clasts, interbeds contain current ripples	${\sim}4cm$ to $7m$ thick, interbeds range from $1cm$ to $0.5m$ thick	High-energy, flowing water within fluvial system
Diamictite facies	Dmm (massive) Dms (stratified)	Clast-poor to clast-rich, muddy, stratified and massive diamictite	Granite, quartz, potassium feldspar clasts, coalified material and root traces common	\sim 10 cm to 3 m thick	High density debris flows
Root-trace-bearing mudrock facies	Mrt	Siltstone, mudstone, and coal	Typically massive, sometimes finely laminated, abundant root traces, thin coal beds, peds, organic debris and intact plant fossils	~5 cm to 5 m thick	Paleosols, overbank floodplain deposits
Heterolithic bioturbated facies	mSb	Heterolithic, very-fine to medium quartz sandstone, siltstone, and mudstone	Sulfur-rich, vertical and horizontal bioturbation, plant material common, may contain micro-hummocky cross stratification	\sim 10 cm to 3 m thick beds, \sim 20 m thick amalgamated packages	Restricted shallow marine or estuarine setting with periodic sediment/organic influx (likely tidally influenced)

Facies codes from Benn and Evans (2010) and Farrell et al. (2012).





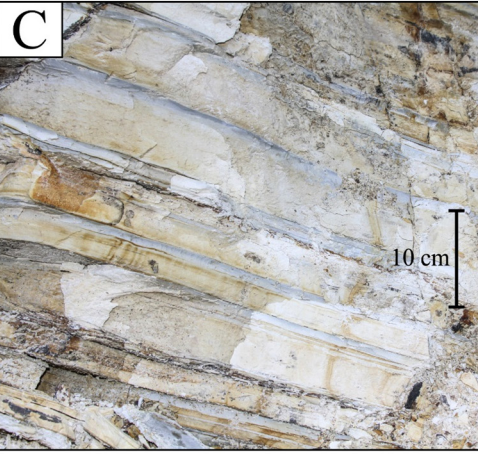


Fig. 4. Sandy conglomerate and breccia facies (Gm/Gp) in core LA-14 and rhythmite facies (Flv) at Location 2. A. Typical weathering profile of Gm/Gp facies in core directly above crystalline basement. B. Rhythmites (tilted) overlying weathered granite basement (also tilted) at Location 2. Contact between basement and rhythmites indicated by white dashed line and white arrow. Rock hammer (28 cm) used for scale. C. ~10 cm rhythmite couplets from the Flv facies in outcrop.

Dadson et al., 2005; Girardclos et al., 2007; Talling, 2014). Outsized clasts are often interpreted as iceberg rafted debris. However, such clasts occur as out runner clast in sediment gravity flows, from vegetational rafting, rock falls off narrow valley walls, anchor ice, and/or due to sea/lake ice rafting (e.g. Bennett et al., 1996; Carto and Eyles, 2012; Dionne, 1993; Doublet and Garcia, 2004; Ferguson, 1970; Garden et al., 2011; Gilbert, 1990; Kempema et al., 2001; Kempema and Ettema, 2011; Postma et al., 1988; Woodborne et al., 1989). Folded rhythmite beds are likely the product of synsedimentary slumping caused by either over-steepening of prograding depositional surfaces (e.g., delta front), over pressurization and fluid expulsion in rapidly deposited sediments, or active tectonism (e.g. Posamentier and Martinsen, 2011). However, discrete faulted zones with vein fill suggest that deformation also occurred following lithification.

5.1.3. Mudrock/fine-grained sandstone facies (Fl/Fm)

The mudrock/fine-grained sandstone facies (Fl/Fm) is \sim 3 cm to \sim 10 m thick (Locations 1 and 3; cores LA-14, CA-53, and AB-06) (Fig. 7A,B,C). It is laterally continuous across outcrops and consists of massive (Fm) to finely laminated (Fl) mudstone, siltstone, and very-fine to fine-grained quartz sandstone. The facies is bounded below by either a sharp or gradational contact. In core AB-06, the Fl/Fm facies consist of black carbonaceous mudstone. At Location 1 (Morro do Papaléo), terrestrial vegetation (ferns, lycophytes, glossopterid and cordaitalean plants) typical of the earliest Permian or latest Carboniferous occur in discrete siltstone beds along with the microplankton *Leiosphaeridia*, which is found in estuarine environments (Fig. 7B,C) (i.e. Guy-Ohlson, 1996; Iannuzzi et al., 2006; Smaniotto et al., 2006). This facies is found in the lower third of the paleovalley fill in association with the rhythmite facies (Flv) and the sandy conglomerate and breccia facies (Gm/Gp). Outside of the paleovalley (Location 3), it is observed overlying the

diamictite (Dmm/Dms) and root-trace-bearing mudrock facies (Mrt).

This facies is interpreted as deposits of stable, low-energy conditions in a lacustrine or estuarine setting. The fine-grained sediments and laminations suggest that settling from suspension into a standing body of water was the dominant form of deposition. Furthermore, the presence of well-preserved intact plant fossils, including some stems found in living position (Iannuzzi et al., 2006), and carbonaceous mudstones also implies a low energy environment with a close proximity to terrestrial vegetation. The presence of one estuarine microplankton element found at Location 1 may suggest a distal connection with a marine environment (i.e. Iannuzzi et al., 2006; Smaniotto et al., 2006).

5.1.4. Cross-stratified sandstone facies (St/Sp)

The cross-stratified sandstone facies (St/Sp) is the most common facies observed at Location 1 and is present in every core that was described (Fig. 8). This facies consists of stacked, erosional-based, lenticular sand bodies (up to 7 m thick and 15 m wide) that incise into each other as well as underlying mudstone, coal, and diamictite beds (Fig. 8A). The sandstones contain scattered pebbles at the base of individual beds as well as medium to coarse-grained sets of trough (St) and planar cross stratification (Sp) (Fig. 8B,C). Interbeds of very-fine to fine-grained cross-laminated/asymmetric current rippled sandstone are present (Fig. 8D). Paleocurrent orientations (cross-stratification; n = 22) from two horizons at Location 1 return mean paleoflow directions of 290 \pm 12° and 223 \pm 10° (1 σ). Stratigraphically, this facies is located in the middle section of the paleovalley fill and occurs in association with the root-trace-bearing mudrock facies (Mrt), the sandy conglomerate and breccia facies (Gm/Gp), and the diamictite facies (Dmm/Dms).

This facies is interpreted as channel bodies within a fluvial system based on the occurrence of cross-stratified beds with normal grading,



Fig. 5. Key features of rhythmite facies (Flv) in cores AB-06 and CA-53. A. Ripples (black arrows) in sandy, bottom portion of couplets, indicating traction between flows and underlying substrate. B. Load and flame structures (black arrows) suggesting rapid loading of unlithified substrate. C. Rip-up clasts of deformed rhythmites in sandstone interbed of Flv facies (black arrow), suggesting traction between flows and underlying substrate. D. Discrete zone of brittle faulting in basal portion of core CA-53, possible evidence for tectonism or failure along delta front.

beds with erosional bases, pebble lags, asymmetric current ripples, and the incised chanelform sand body geometries seen in outcrop. Cross-stratified beds are diagnostic of bedload dominated flows and sand body geometries indicate channelization. Paleoflow orientations at Location 1 are indicative of transport towards the center and down the axis of the paleovalley. The close association with the root-trace-bearing mudrock facies (Mrt), which contains clay-rich paleosols, coal beds, and in-situ plant fossils, is evidence for a terrestrial environment. Stacked sand bodies that are floored by an unconformity and incise into each other occur in the basal portion of this facies. This suggests that the channels migrated in a setting with low accommodation space and may be part of a lowstand systems tract (e.g. Martinsen et al., 1999).

5.1.5. Diamictite facies (Dmm/Dms)

The diamictite facies (Dmm/Dms) beds are up to 3 m thick and consist of stacked, en echelon-like, lenses and wedge-shaped bodies composed of massive (Dmm) to crudely stratified (Dms), clast-poor to clast-rich, muddy, matrix-supported diamictite (Locations 1 and 3; Cores LA-14, RN-10, and AB-06). On outcrops, individual diamictite bodies have sharp to erosional bases. Dmm/Dms beds thin and pinch out over a few tens of meters and, at Location 3, the diamictite onlaps igneous basement rocks (Fig. 9). Clasts are angular to subangular and consist of quartz, feldspar, and highly weathered granite granules and pebbles. Meter-scale lenses of clast-supported conglomerate sometimes occur within the diamictites, as do thin coal lenses (Fig. 10A). Mudstones with root traces and coal beds (Mrt) frequently overlie the diamictite beds (Fig. 10B,C). Mudstone, siltstone, and coal rip-up clasts up

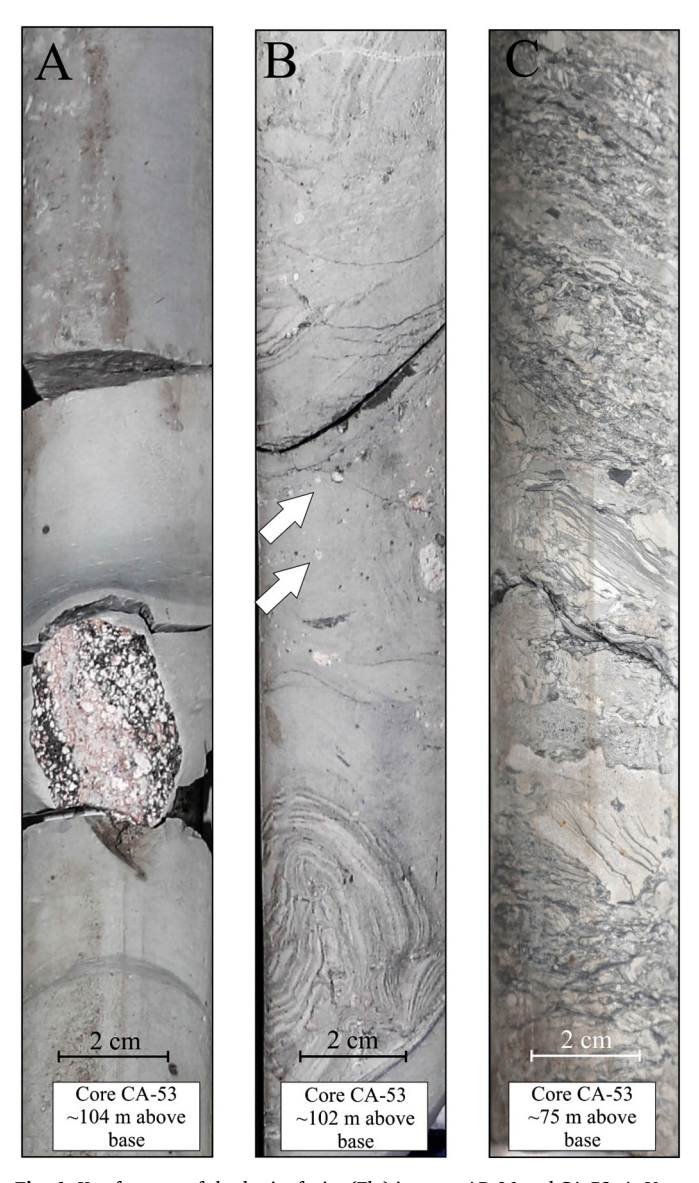


Fig. 6. Key features of rhythmite facies (Flv) in cores AB-06 and CA-53. A. Very rare example of lonestone. B. Folded and faulted rhythmites from syndepositional brittle (faulting) and ductile deformation (slumping). White arrows indicate small granule and pebble sized clasts occurring along bedding planes. C. Brecciated and sheared rhythmites, possible evidence for tectonism or failure along delta front.

to 30 cm in length are also common in the Dmm/Dms facies (Fig. 10D). The internal fabric, including the A axes of clasts, is sub-horizontal and parallel to bedding. Siltstone rafts with soft sediment deformation are also observed in Dmm/Dms beds (Fig. 10E). This facies is located in the middle section of the paleovalley fill as well as outside the paleovalleys and occurs in association with the cross-stratified sandstone facies (Sp/St), the sandy conglomerate and breccia facies (Gm/Gp), and the root-trace-bearing mudrock facies (Mrt).

The Dmm/Dms facies is interpreted as high density debris flows deposited on alluvial fans and fan deltas. This determination is based on the occurrence of stratified and bedded diamictites, coal and siltstone rip-up clasts, soft-sediment deformation, the internal bedding-parallel fabric, and erosive or sharp lower contacts. Matrix-supported beds with a strong bedding-parallel fabric suggest that a high density fluid is responsible for sediment transport (e.g. Enos, 1977). Stacked, en echelon beds observed in the Dms facies at Location 3 support successive high density flows or surges that have piled into and overridden previous







Fig. 7. Mudrock/fine-grained sandstone facies (Fl/Fm) in outcrop. A. Laminated siltstone (Fl facies) beds at Location 3. Rock hammer (28 cm) for scale. B. *Botrychiopsis* fossil from top of the Fl facies at Location 1. C. *Glossopteris* fossil from top of Fl facies at Location 1.

flows or surges. The isolated lenses of clast-support with normal grading are zones of low viscosity fluidized flow within the overall high viscosity debris flow. Thin coal lenses, coal rip-up clasts, the association with root-trace-bearing mudrock facies, and root traces that occur on the top of diamictite beds is evidence for deposition in a humid subaerial environment.

5.1.6. Root-trace-bearing mudrock facies (Mrt)

The root-trace-bearing mudrock facies (Mrt) (Location 1 and 3; all cores) consists of laterally continuous, 5 cm to 5 m thick, root-trace-bearing, massive or (less commonly) laminated mudstone and siltstone beds (Figs. 10C and 11A, B). This facies also contains poorly-developed, low-grade coal beds up to 2 m thick with intercalated mudstone and siltstone laminations (Fig. 10C). Rocks of this facies rest on sharp or gradational lower contacts and are occasionally cut by overlying diamictite beds or channel-form, cross-stratified sandstone bodies. Claylined root traces, mud cracks, intact and disaggregated plant remains, slickensides, and wedge shaped peds, are all common throughout this facies (Fig. 11A, B). Mudrock in this facies occur in the middle section of the paleovalley fill in association with the cross-stratified sandstone facies (St/Sp), the sandy conglomerate and breccia facies (Gm/Gp), and the diamictite facies (Dmm/Dms).

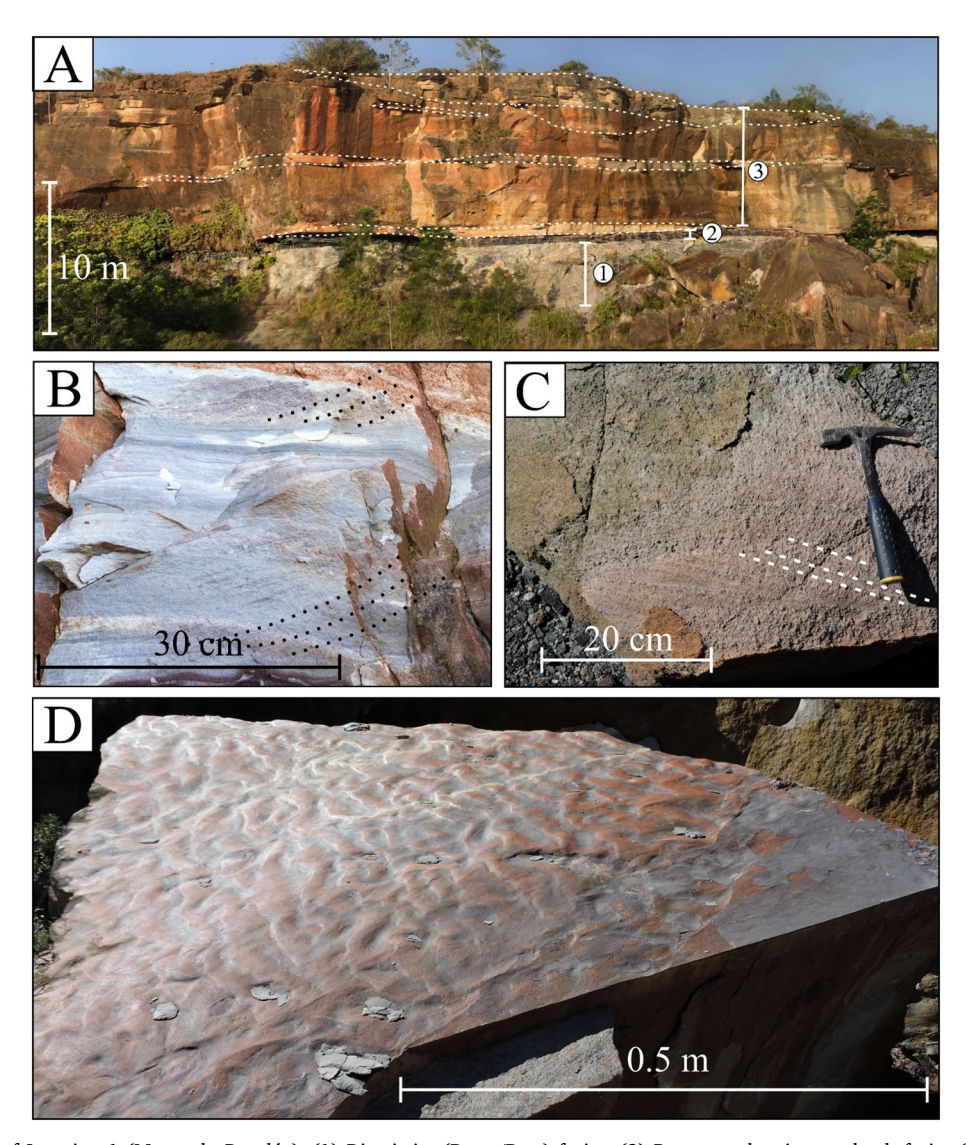


Fig. 8. A. Photomosaic of Location 1 (Morro do Papaléo). (1) Diamictite (Dmm/Dms) facies. (2) Root-trace-bearing mudrock facies (Mrt). (3) Cross-stratified sandstone facies (St/Sp). Channel body geometries within St/Sp facies outlined by dashed white lines. B. Trough cross beds from St facies at Location 1 indicated by black dashed lines. C. Planar cross beds from Sp facies at Location 1 indicated by white dashed lines. D. Rippled bedding surface at Location 1.

This facies is interpreted as overbank floodplain deposits from within a fluvial-dominated valley and incipient paleosols that formed on top of fan deltas. The association with erosional sand bodies from the cross-stratified sandstone (St/Sp) facies suggests proximity to fluvial channels that experienced base level fluctuations. Furthermore, the wedge-shaped peds, mud cracks, slickensides, and clay-lined root traces are typical of vertisols that formed on crevasse splays/floodplain sediments and experienced shrinking and swelling from episodic wetting and drying (e.g. Gustavson, 1991). Massive mudstone and siltstone beds were likely deposited during flooding and were subsequently bioturbated by vegetation, giving them a homogenous appearance. Coal beds and fossil plant fragments are also indicative of a flooded, anoxic terrestrial setting such as a floodplain that allowed for intervals of peat accumulation. The discontinuous and poorly developed nature of the coals, along with the presence of clastic laminations and interbeds, are consistent with coals that formed over relatively short intervals of time due to repeated flooding.

5.1.7. Heterolithic bioturbated facies (mSb)

Heterolithic bioturbated facies (mSb) packages are up to $20\,\mathrm{m}$ thick and consist of laterally continuous beds ($<3\,\mathrm{m}$ thick) of mudstone, siltstone, and very-fine to medium-grained quartz sandstone (Cores LA-

14, IB-94, and RN-10). Beds typically display bioturbation levels from 2 to 3 on the Droser and Bottjer (1986) ichnofabric index. The beds have sharp or gradational lower contacts and sharp or gradational upper contacts. Beds contain both horizontal and vertical traces of *Gyrolithes* and *Teichichnus*. *Teichichnus* traces are retrusive with concave-up spreite (Fig. 11D). The facies also contains medium-grained, micro-hummocky cross-stratified sandstone, rhythmites with alternating fine-grained sandstone and crinkled or wavy carbonaceous muddy laminae (Fig. 11C), and discrete mudstone beds containing coalified organic debris and disaggregated fossil plant fragments. Sulfur occurs in beds throughout this facies. Deposits of the mSb facies occur in the upper third of the paleovalley fill.

This facies represents restricted marine or estuarine deposits that accumulated above storm wave base with episodic influxes of coarse-grained sediment and plant/organic matter. The occurrence of sulfurrich beds with *Teichichnus* and *Gyrolithes* suggest a restricted, marine influenced depositional environment. Discrete beds containing abundant plant fragments, micro-hummocky cross-stratification, and alternating mud and sand laminae are evidence for episodic high energy storm beds or possible tidal influence within an overall low-energy environment. *Teichichnus* traces with retrusive spreite also suggest that organisms moved upward through the substrate to adjust to an episodic

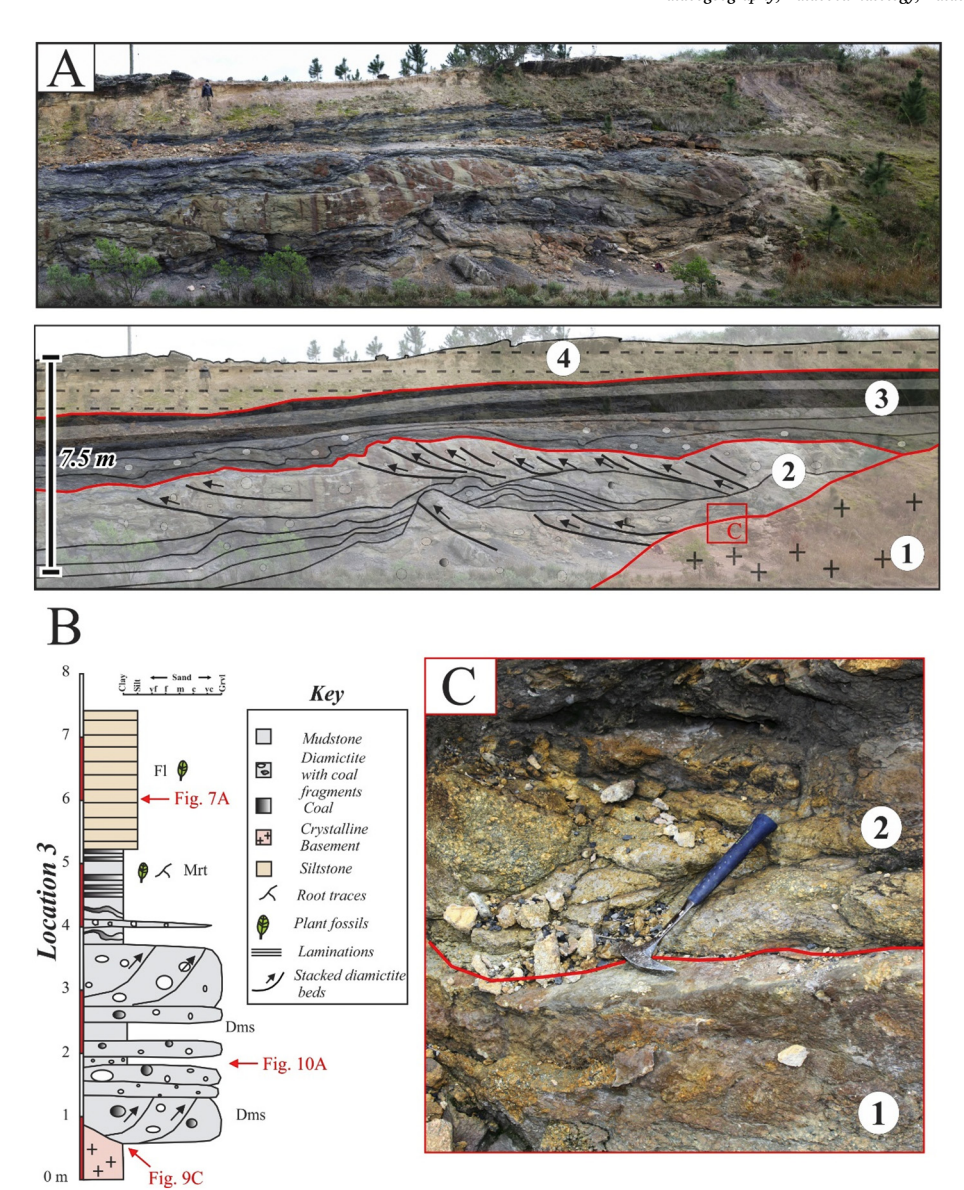


Fig. 9. A. Photomosaic of Location 3. Red solid lines are contacts between facies and black lines with arrows are stacked diamictite beds. (1) Granite basement. (2) Diamictite (Dms) facies. (3) Root-trace-bearing mudstone (Mrt) facies. (4) Mudrock/fine-grained sandstone (Fl) facies. B. Stratigraphic column of Location 3. C. Location 3 contact between unpolished/unstriated granite basement (1) and onlapping Dms facies (2) indicated by red solid line. Rock hammer (28 cm) for scale. (For interpretation of the references to colour in this figure legend, the reader is referred to the web version of this article.)

influx of coarser sediment.

5.2. Stratigraphy

A longitudinal section of the paleovalley system was created using a combination of core and outcrop measurements (Fig. 12). The lowermost coal bed in each core or outcrop was used as a datum since these are interpreted to indicate an increase in accommodation (clastic starved conditions) following the development of a regional unconformity (e.g. SB-3; Holz, 2003; Holz et al., 2006; changed to SB-4 in Holz et al., 2010). Individual facies show a high degree of vertical and horizontal variability within the paleovalleys and cannot be traced across the entire length of the longitudinal profile. Furthermore, abrupt changes in basement relief and sediment thickness are indicated from the core data and supported by resistivity measurements collected by Tedesco et al. (2016). These sharp variations in basement topography correspond closely to the location of faults mapped by the Brazilian Geologic Survey (CPRM) (Fig. 12). The sandy conglomerate and breccia facies, rhythmite facies, and mudrock/fine-grained sandstone facies

occur in the lower portion of the paleovalley system fill within the paleotopographic lows (Fig. 12). The cross-stratified sandstone facies, sandy conglomerate and breccia facies, diamictite facies, and root-trace-bearing mudrock facies coexist in the middle section of the paleovalley system fill and are thicker to the southeast, away from the Paraná Basin (Fig. 12). The heterolithic bioturbated facies occurs in the upper portion of the fill and is thickest in the northwestern portion of the Leão Paleovalley near the margin of the Paraná Basin and thins towards the southeast (Fig. 12).

5.3. Detrital zircon (U-Pb) geochronology results

Detrital zircon samples were collected from a medium, pebbly, quartz-rich sandstone bed (Gm/Gp facies) \sim 0.5 m above basement in the basal section of the paleovalley fill (sample MP, Location 2) and a medium, quartz-rich sandstone bed (St/Sp facies) in the middle section of the paleovalley fill (sample MDP6, Location 1) (Fig. 13). Sample MP was from a unit previously interpreted as the Itararé Gp., and sample MDP6 was from a unit previously interpreted as the Rio Bonito Fm. (e.g.

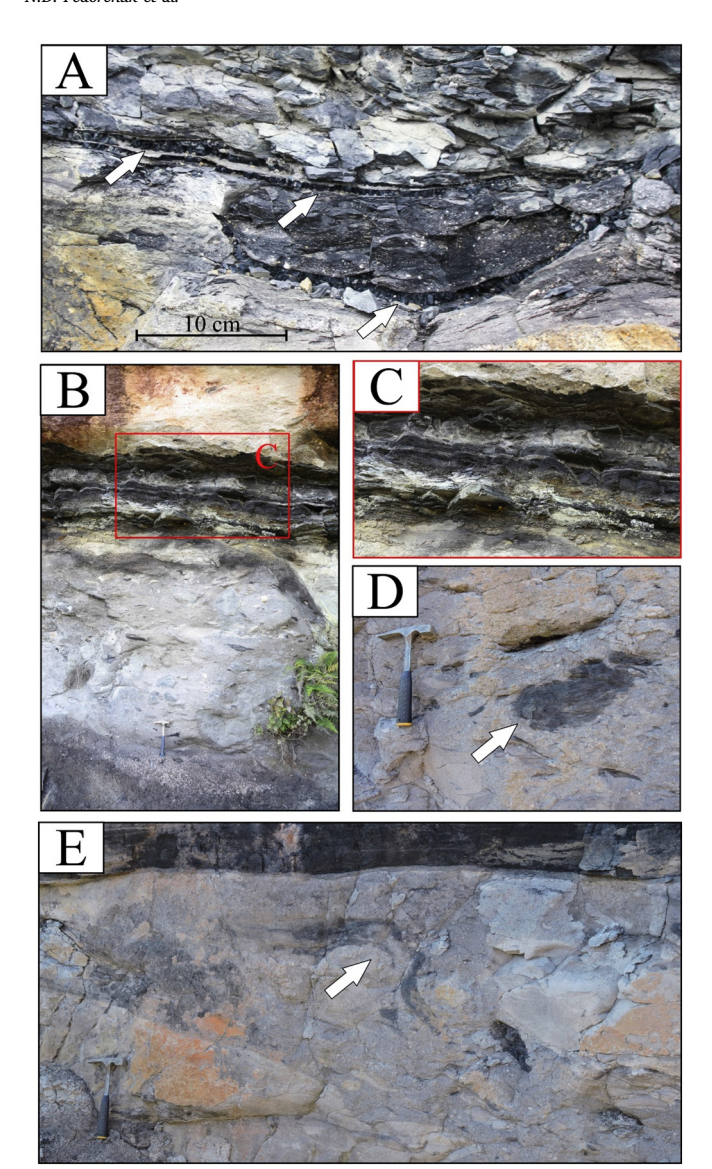


Fig. 10. A. Thin coal lenses in the diamictite (Dms) facies at Location 3. B. Outcrop at Location 1 with root-trace-bearing mudrock facies overlying the diamictite facies (Dmm). Rock hammer (28 cm) for scale. C. Root-trace-bearing mudrock facies. D. Carbonaceous siltstone rip-up clast in Dmm facies at Location 1. Rock hammer (28 cm) for scale. E. Soft-sediment deformation of siltstone raft in Dmm facies at Location 1. Rock hammer (28 cm) for scale.

Iannuzzi et al., 2006; Smaniotto et al., 2006; Tedesco et al., 2016). Both samples were found to contain a single (unimodal) population of Neoproterozoic grains (c. 800–550 Ma) (Fig. 14). U-Pb data for these samples can be found in the supplemental data files. Kernel density estimate (KDE) plots show strongly overlapping peaks at $\sim\!595\,\mathrm{Ma}$ (MDP6) and $\sim\!605\,\mathrm{Ma}$ (MP) (Fig. 14). A comparison of the two samples using a Komogorov-Smirnoff (K-S) test yielded a P-value of 0.191, indicating that there is a >95% probability zircon populations from the two samples are not significantly different (i.e. P-value >0.05).

6. Discussion

Three distinct facies associations were observed that correspond to the lower, middle, and upper section of the paleovalley fill. These are a lacustrine/estuarine facies association in the basal portion of the paleovalleys, a fluvial-dominated facies association in the middle section, and a restricted marine/estuarine facies association in the upper portion. None of these contained any evidence of glacially-influenced

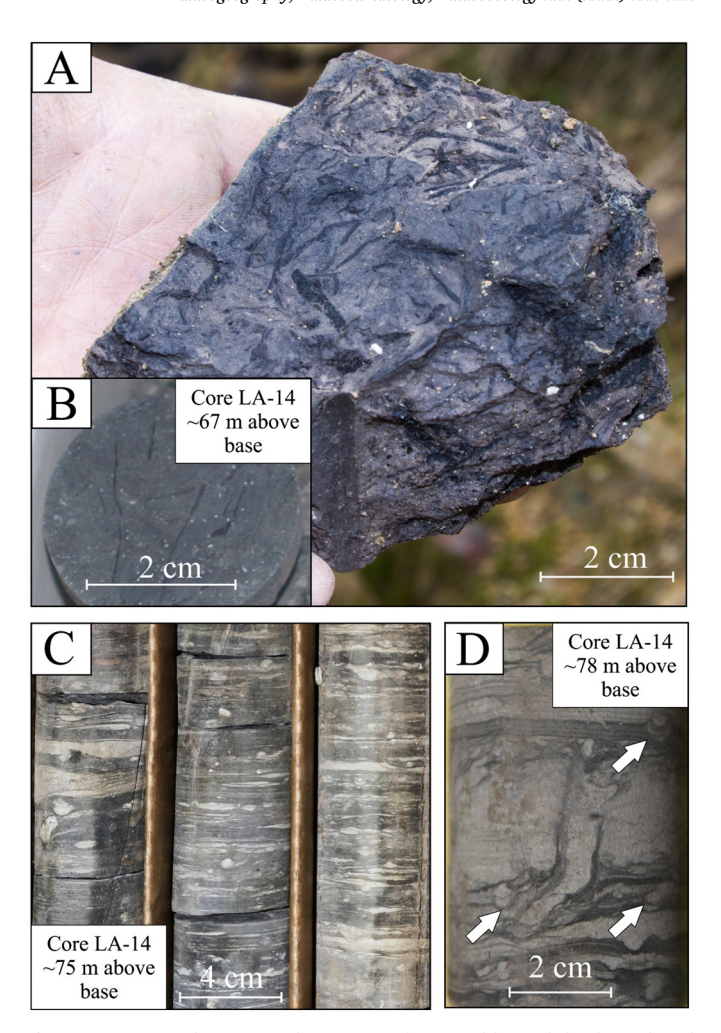


Fig. 11. Root-trace-bearing mudstone (Mrt) facies and heterolithic bioturbated (mSb) facies. A. Root traces within Mrt facies at Location 3. B. Root traces within Mrt facies in core LA-14. C. Heterolithic bioturbated beds in core IB-94. D. Bioturbation with concave-up spreite (white arrows) in core LA-14.

deposition. Additionally, detrital zircon geochronology results demonstrate that the Mariana Pimentel and Leão Paleovalleys were internally drained and do not contain extra-basinal sediments that were derived from an ice center over Africa.

6.1. Lacustrine/estuarine facies association

The bottom portion of the paleovalley fill is significant to this study because it has been previously interpreted as the glaciogenic Itararé Gp. based on the presence of rhythmites and poorly sorted sediments. This implies that the sediments were deposited in a temperate, glacial fjord (e.g. Iannuzzi et al., 2006; Tedesco et al., 2016). However, these sediments are interpreted here as having been deposited in several isolated, non-glacial lacustrine basins or a single estuarine system with internal sub-basins connected to the Paraná Basin (Fig. 15A). This corresponds to a facies association of the sandy conglomerate and breccia facies (Gm/Gp), the mudrock/fine-grained sandstone facies (Fl/Fm), and the rhythmite facies (Flv). These sediments would be temporally equivalent to the Triunfo and Paraguaçu Mbrs., which are defined as the basal-to-middle portion of the Rio Bonito Fm. (Fig. 3).

The Gm/Gp facies is consistent with alternating sheet flow and mass transport from an alluvial fan/fan delta system on the steep margins of a lacustrine/estuarine basin. The in-situ weathering of crystalline basement, which grades into conglomerate and breccia, combined with the immature sediment composition, angular (non-striated) clasts, and

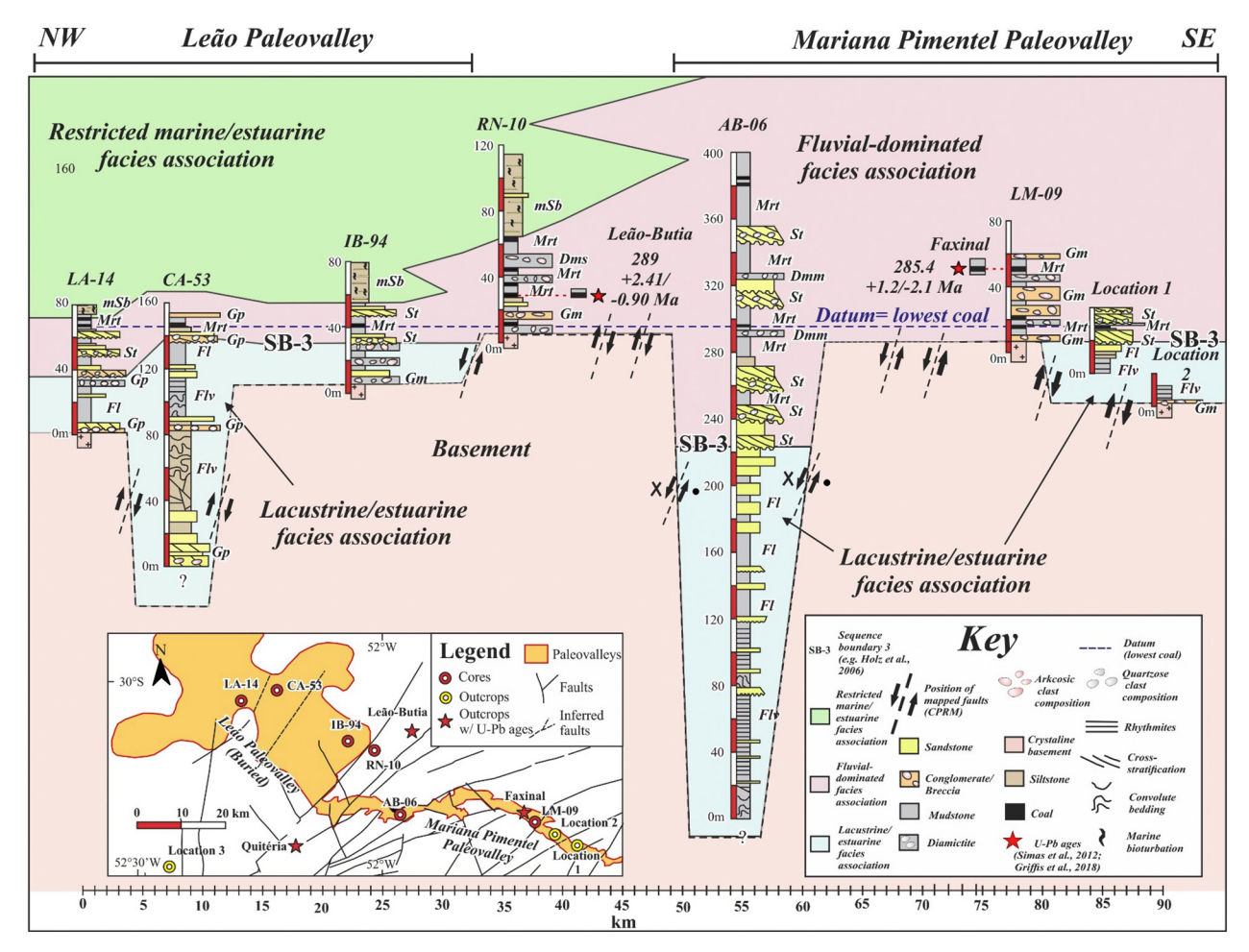


Fig. 12. Cross section of Mariana Pimentel and Leão paleovalleys. Vertical exaggeration is 140 × and datum (dashed blue line) is based on lowermost coal beds. U-Pb ages (red stars) are from Griffis et al. (2018) and Simas et al. (2012). (For interpretation of the references to colour in this figure legend, the reader is referred to the web version of this article.)

poor sorting, suggest sediment was shed directly off the subaerially exposed paleovalley walls and was not glacially transported. The cross section indicates that the alluvial fan sediments are thickest near or on top of fault-bounded, raised basement blocks (Fig. 12). The weathering profile in the Gm/Gp facies implies that bedrock was exposed to chemical weathering for an extended duration of time. This is not what would be expected in a fjord environment where glacial erosion would rapidly remove weathered bedrock, producing a scoured bedrock surface beneath sediment fill (e.g. Syvitski et al., 1987). Furthermore, interbeds from these alluvial fan sediments, which contain root traces and coalified organic matter imply that the alluvial fans/fan deltas existed in a humid, vegetated setting rather than in a glacially influenced fjord.

Rhythmites (Flv facies) and fine-grained, laminated rocks (Fl/Fm facies) are found within fault-bounded, sub-basins (high accommodation zones; Fig. 12) that may have started as separate, small lacustrine basins. The mixture of terrestrial flora and rare estuarine microplankton elements described by Iannuzzi et al. (2006) and Smaniotto et al. (2006) from fine-grained rocks near the top of the lacustrine/estuarine facies association (base of Location 1) indicate a possible marine inundation of these basins. This is likely due to the transgression of the "Paraguaçu Sea" (Fig. 3). Although a transition from a lacustrine to estuarine setting is hypothesized, there is no marker bed or facies change that clearly marks this change across the paleovalley(s). However, in core AB-06, there is gradual shift from thick rhythmites (Flv facies) to thinner rhythmites and carbonaceous mudstone of Fl facies. This may represent a gradual progression from more proximal to distal hyperpycnal flows associated with a marine transgression.

The Flv facies is interpreted as turbidites or hyperpycnites in which flows were triggered by floods, failure along a prograding delta front, or sediment shed during intermittent tectonic activity. In tidewater fjords, buoyant meltwater typically forms an overflow plume as it rises to the surface over denser saltwater (e.g. Cowan and Powell, 1990; Mugford and Dowdeswell, 2011; Powell, 1990). The rhythmites observed in the Mariana Pimentel and Leão Paleovalleys appear to be the product of underflows rather than rain-out from overflow plumes. Although hyperpycnal flows and turbidites are also important depositional processes in fjords due to the high sedimentation rates and steep slopes (e.g. Ó Cofaigh and Dowdeswell, 2001; Powell, 2003; Syvitski et al., 1987), they also occur in almost any depositional environment where a riverine-introduced, dense sediment-water admixture is transported as underflows down a slope and, therefore, are not diagnostic of glacial meltwater sedimentation (e.g. Zavala and Arcuri, 2016). This highlights the important distinction that not all rhythmites in the Paraná Basin are glaciogenic, and some may be temporally equivalent to the post-glacial Rio Bonito Fm. In general, rhythmic sediments across the Paraná Basin could be the product of annual or seasonal lake processes (i.e. true varves), surge-like turbidites, or tidal activity among other cyclical processes (e.g. Ó Cofaigh and Dowdeswell, 2001; Schimmelmann et al., 2016; Zavala and Arcuri, 2016; Zolitschka et al., 2015).

Another line of evidence that was previously used to support a glaciogenic interpretation of the Mariana Pimentel and Leão Paleovalleys is the presence of rare dropstones contained within the rhythmite facies. However, as discussed earlier, dropstones commonly occur in non-glacial environments due to processes such as rock falls off

Location 1 (Morro do Papaleo) 50 45 Fig. 8D Fig. 8A 40 35 10B,C,D,E 30 25 Key Fig. 8C Sample Detrital zircon Sandstone SB-3 sample 20 Ripples Siltstone Root traces Mudstone 15 Fm Plant fossils Diamictite with coal Fm Trough cross fragments beds 10 Laminations Crystalline Planar cross basement 5 beds FI Figs. 7B,C Sequence Cover boundary 3 Location 2 5 km

Fig. 13. Stratigraphic columns from Location 1 (Morro do Papaléo) and Location 2 with detrital zircon sample locations indicated by red stars (column after Iannuzzi et al. (2006); Smaniotto et al. (2006)). (For interpretation of the references to colour in this figure legend, the reader is referred to the web version of this article.)

Fig. 4C

5

of narrow valley walls, or rafting by lake ice, vegetation, or riverine/lacustrine anchor ice (e.g. Bennett et al., 1996; Dionne, 1993; Doublet and Garcia, 2004; Ferguson, 1970; Garden et al., 2011; Gilbert, 1990; Kempema et al., 2001; Kempema and Ettema, 2011; Woodborne et al., 1989). Thus, the presence of exceedingly rare (only 2 observed in > 800 m of core, none in outcrop) and isolated dropstones is not in and of itself indicative of a glacially-influenced environment. The outsized clasts observed in this study have lithologies consistent with the underlying basement. Furthermore, there are no associated clast clusters (iceberg dump structures), diamictite pellets, or ice-keel marks, which are commonly found in the ice rain-out facies of temperate fjords (e.g. Dowdeswell et al., 1993; Powell, 2003). Granule and pebble sized clasts that occur along discrete bedding planes and associated with other coarse sediment are interpreted here as small debris flows rather than

as dropstones (e.g. Postma et al., 1988).

Finally, when tidewater glaciers retreat from a fjord they tend to calve rapidly across deep sub-basins and stabilize on shallow and narrow "pinning points", often located on bedrock sills (e.g. Cowan et al., 2010; Molnia, 1983; Syvitski et al., 1987). Here, the rate of calving is reduced and they are able to maintain temporary ice-balance equilibrium. The sills and proximal parts of adjacent basins typically have evidence of subglacial abrasion, trapped icebergs (keel marks), morainal bank build-up, and grounding line fan sedimentation (e.g. Cowan et al., 2010; Ottensen and Dowdeswell, 2009; Syvitski et al., 1987). Sediments deposited in the deep sub-basins, located in front of the sills, will show abundant evidence of ice-rafted debris, turbidity currents, and plume rain-out (e.g. Powell, 2003; Syvitski et al., 1987). Contradicting this model, cores (LM-09, IB-94, LA-14) located on

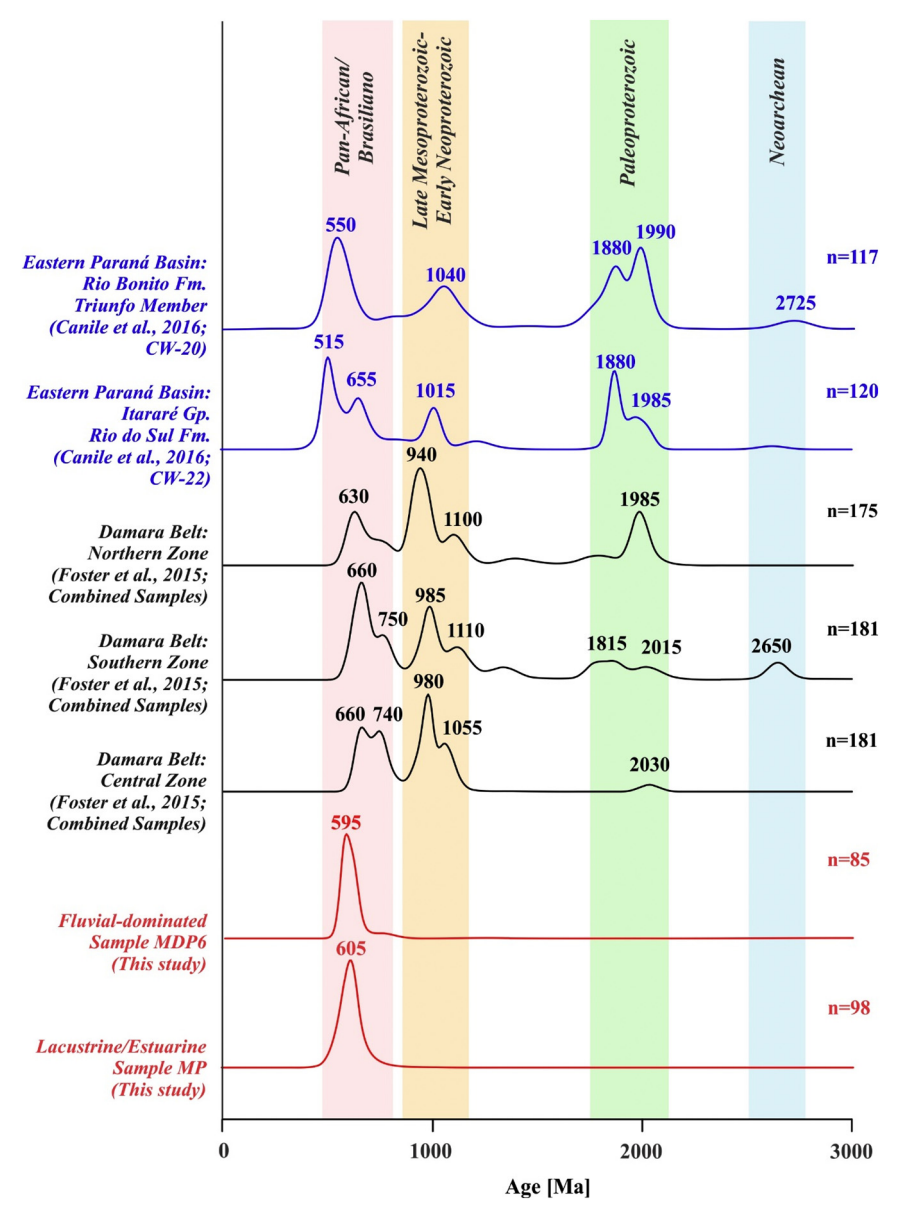


Fig. 14. Detrital zircon results from Mariana Pimentel Paleovalley. Kernel density estimates for samples MP and MDP6 (red; this study) compared to the Damara belt in Namibia (black; Foster et al., 2015) and the eastern margin of the Paraná Basin (blue; Canile et al., 2016). (For interpretation of the references to colour in this figure legend, the reader is referred to the web version of this article.)

bedrock highs within the Mariana Pimentel and Leão Paleovalleys show a weathering profile in igneous and metamorphic basement that grades into the sandy conglomerate and breccia facies (humid alluvial fan deposits) and root-trace-bearing mudrock facies (coal-bearing floodplain deposits). No grooves or striations were observed on basement surfaces and no striated, faceted, or exotic clasts were observed as would be expected in ice proximal basins. As previously described, cores from within the deep sub-basins (AB-06, CA-53) do not show any evidence of plume rain-out (overflows) or abundant ice-rafted debris, as would be expected < 10 km in front of pinning points (e.g. Powell, 2003).

6.2. Fluvial-dominated facies association

The middle portion of the paleovalley fill is interpreted here as lowstand fluvial-dominated sediments of the Rio Bonito Fm. (equivalent to the Sideropolis Mbr.) (Figs. 3 and 15B). Tonsteins from this facies association are used to place the paleovalley system within a broader stratigraphic context. The fluvial-dominated facies association

contains the cross-stratified sandstone facies (St/Sp), the sandy conglomerate and breccia facies (Gm/Gp), the diamictite facies (Dmm/Dms), and the root-trace-bearing mudrock facies (Mrt). The St/Sp facies is interpreted as fluvial channels and the Mrt facies represents overbank floodplain and peat deposits. The poorly-developed, discontinuous nature of the coal seams in the Mariana Pimentel paleovalley is consistent with episodic flooding along a lowstand fluvial system rather than a more prolonged interval of standing water. The Dmm/Dms facies has the characteristics of muddy debris flows that are derived from the valley slopes. The fact that the Dmm/Dms facies also occurs at Location 3, outside of the paleovalleys where it onlaps granite basement, suggests paleotopographic relief outside of the paleovalleys as well.

A drop in base level within the lacustrine/estuarine system, occurring at the base of the St/Sp facies, allowed the fluvial-dominated facies association to extend out into the Paraná Basin. We correlate this drop in base level in the study area to SB-3 (Fig. 3; e.g. Holz, 1999, 2003) rather than SB-2 (contact between Itararé Gp. and Rio Bonito Fm.) because tonsteins within the paleovalleys have been radiometrically dated by Simas et al. (2012) and Griffis et al. (2018) to ~8 and 12 Myr

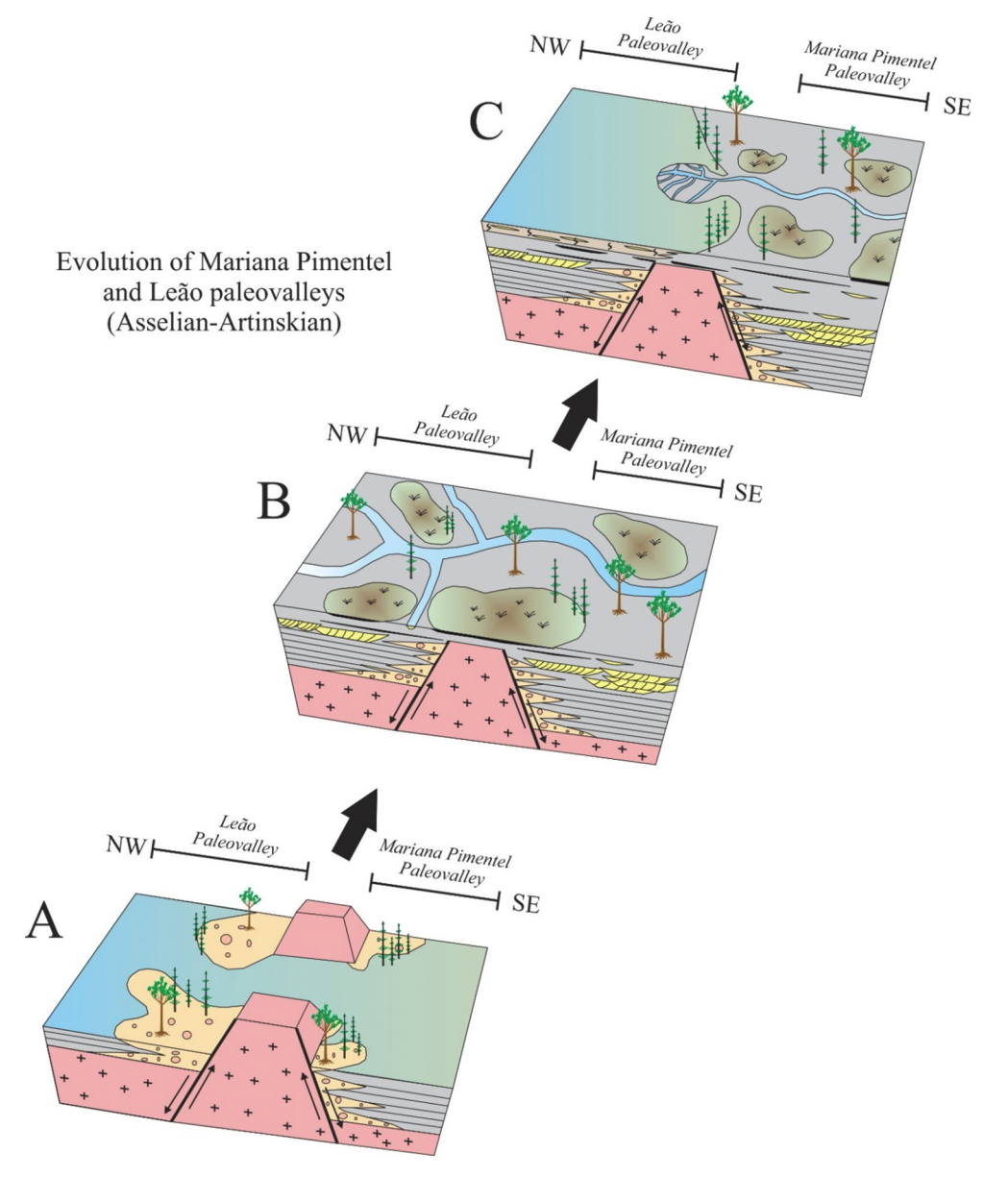


Fig. 15. Block diagrams showing evolution of Mariana Pimentel and Leão paleovalleys during early Permian. A. Lacustrine/Estuarine facies association. B. Fluvial-dominated facies association. C. Restricted marine/estuarine facies association.

younger than the coals from the base of the Rio Bonito Fm. (located outside of the paleovalleys) and because there is no evidence for glaciation within the basal fill of the paleovalleys. It should be noted that Holz et al. (2006) related SB-3 to tectonism on other areas of the RGS. The fact that younger coals exist within the paleovalleys below the paleotopographic level of older coals (such as those at Quitéria; Fig. 1C) located outside of the paleovalley supports the interpretation that base level fell, and incision occurred after the older coals were deposited.

6.3. Restricted marine/estuarine facies association

The top portion of the paleovalley fill is interpreted as a restricted marine/estuarine environment (Fig. 15C). It is comprised of the heterolithic bioturbated facies (mSb). This facies association is thickest near the northwestern (basinward) portion of the Leão Paleovalley and pinches out near the connection with the Mariana Pimentel Paleovalley. This bioturbated facies association represents a marine transgression of the "Palermo Sea" (Fig. 3) into the Leão Paleovalley. The mSb facies has the characteristics of a low-energy restricted marine or estuarine

environment in which sediment settled from suspension. This setting experienced episodic input of coarse sediment from either tidal action or storms. Coals seams located near the connection of the Mariana Pimentel and the Leão Paleovalley contain sulfur, suggesting an interaction between the fluvial-dominated setting and the estuarine environment in this location.

6.4. Detrital zircon geochronology

The unimodal zircon population ranging from c. 800–550 Ma in both the basal lacustrine/estuarine facies association and the overlying fluvial-dominated facies association suggests that the sediment source area remained unchanged throughout deposition within the paleovalleys. This age range is consistent with magmatic events that occurred during the Neoproterozoic Pan-African/Brasiliano tectonic cycle. In particular, the ages are nearly identical to the igneous and metamorphic basement of the Pelotas Batholith (part of the Dom Feliciano Belt; ~820–580 Ma) that the paleovalleys directly overlie, indicating a local source (e.g. Babinski et al., 1997; Cordani et al., 2000; Gastal et al.,

2005; Leite et al., 2000; Philipp and Machado, 2005; Saalmann et al., 2011; Silva et al., 1999). Possible igneous and metamorphic sources from the underlying Pelotas Batholith include: the Capão do Leão Granite, the Encruzilhada do Sul Intrusive Suite, the Arroio Moinho Granite, the Pinheiro Machado Suite, the Cordilheira Metagranite, the Quitéria Metagranite, and the Piratini gneiss (e.g. Gastal et al., 2005). All of these sources have ages that closely overlap the zircon populations identified from the paleovalley fill (e.g. Gastal et al., 2005; Silva et al., 1999).

These results can be contrasted to detrital zircon samples analyzed by Foster et al. (2015) from Neoproterozoic sedimentary and metasedimentary rocks across the Damara Belt in central Namibia (Fig. 14). The Damara Belt is interpreted to have been adjacent to the RGS during the Carboniferous and Permian so that any glaciers emanating out of Africa would have drained across this area (Fig. 1B) (e.g. de Wit et al., 2008). Conspicuously absent in the detrital zircon samples from the paleovalleys is the presence of late Mesoproterozoic to early Neoproterozoic (~1200-900 Ma) ages that are prevalent in all of the Damara Belt samples (Fig. 14) (Foster et al., 2015). There is no source of equivalent Mesoproterozoic to early Neoproterozoic grains in southern Brazil, making this age range a useful indicator of African provenance. Paleoproterozoic and Neo-Archean ages are also present in Damara Belt samples but absent from the paleovalleys (Foster et al., 2015). Furthermore, Itararé Gp. and Rio Bonito Fm. detrital zircon samples collected on the eastern margin of the Paraná Basin show strong Mesoproterozoic, Paleoproterozoic, and Neo-Archean peaks that have been interpreted to represent African sources (Fig. 14) (e.g. Canile et al., 2016). This demonstrates that, unlike the eastern margin of the Paraná Basin, the paleovalleys examined here on the RGS were internally drained with no direct connection to Africa. Hypothetically, even if glacial sediments were deposited in this region and were subsequently eroded and resedimented during post-glacial times, we would still expect African zircons to be present in the fluvial sandstones but they were not detected.

6.5. Origin of the Mariana Pimentel and Leão paleovalleys

Multiple lines of evidence support the interpretation that the Mariana Pimentel and Leão Paleovalley system was formed by the reactivation of older basement structures during the Carboniferous and early Permian. This includes: (1) abrupt changes in sediment thickness, vertical and lateral facies changes, as well as the discontinuous nature of individual facies within the paleovalleys that correspond closely to the location of mapped faults (Fig. 12), (2) the position of the paleovalleys within a bend and offset in the major NE-SW trending Neoproterozoic Dorsal do Canguçu Shear Zone (Fig. 1C) (e.g. Fernandes and Koester, 1999; Passarelli et al., 2011; Philipp and Machado, 2005), (3) discrete zones of faulting and slumping within rhythmites and finegrained sediments from the basal portion of the paleovalleys (Figs. 5 and 6), (4) coarse-grained, immature sediments such as conglomerates, breccias, and diamictites with coal clasts (alluvial fan sediments) that onlap basement and are thickest near mapped faults (Fig. 12), (5) the drop in base level between the basal lacustrine/estuarine facies association and the overlying fluvial-dominated facies association, corresponding to a tectonically-related regional sequence boundary (Fig. 3; SB-3) (Holz et al., 2006) to which an angular unconformity on some areas of the RGS is associated, and finally (6), apatite fission track analysis of the Pelotas Batholith conducted by Oliveira et al. (2016) is suggestive of basement uplift and reactivation of faults on the NE part of the RGS during the Permian.

The reactivation of faults across the Paraná Basin, including the RGS, during the Carboniferous and Permian has been described by multiple authors and attributed by some to accretion on the southern margin of Gondwana (Gondwanides or San Rafael Orogeny) (e.g. Holz et al., 2006; Kleiman and Japas, 2009; Oliveira et al., 2016; Trzaskos et al., 2006). Furthermore, the correlation between the Mariana

Pimentel and Leão Paleovalleys and basement structures has been discussed in previous studies. Holz (2003) and Tedesco et al. (2016) both noted that the borders of the paleovalleys correspond closely to known faults. Guerra-Sommer et al. (2008b) and Ribeiro et al. (1987) indicate that the thickest coal deposits in the paleovalleys occur within downthrown basement blocks controlled by a NE trending fault system.

The position of the Mariana Pimentel Paleovalley within the DCSZ and the facies assemblage of the paleovalley are both consistent with the evolution of a small tectonically controlled basin or basins. The thickest sedimentary fill within the paleovalley (core AB-06) corresponds to a major bend and offset in the master faults of the DCSZ (Fig. 12). Releasing bends in such systems form a zone of separation between parallel strike-slip master faults, which can nucleate small pull-apart basins. Such basins are common along reactivated older faults in rigid intracratonic settings. Basin fill is often comprised of lacustrine facies and pro-deltaic facies that form on down-dropped grabens (towards the fault with the most slip) and alluvial fan/fan delta sedimentation on basin margins (e.g. Hempton and Dunne, 1984; Sarp, 2015; Waldron, 2004). Rhythmic, underflow sediments of non-glacial origin are common within these basins (e.g. Hempton and Dunne, 1984; van der Lingen and Pettinga, 1980). It is common for separate lacustrine sub-basins to evolve into a fluvial valley (e.g. Hempton and Dunne, 1984; Kwon et al., 2011; Waldron, 2004). There are also examples of these features being inundated by marine waters, creating estuaries (e.g. Ysufoğflu, 2013). A tectonic origin for the Mariana Pimentel and Leão paleovalley system during the Carboniferous and early Permian, would explain why the coal seams within the paleovalleys are younger than transgressive coals found across the RGS uplands (e.g. Griffis et al., 2018).

The unusually wide shape and shallow depth of the Mariana Pimentel paleovalley was characterized in detail by Tedesco et al. (2016). It was interpreted as an eroded (truncated) U-shape, which is more characteristic of a glacially carved valley, rather than a V-shaped fluvial valley. However, modern fluvial systems often flow down the axes of pull-apart basins such as the Anatolian Fault system in Turkey, and these basins often have depth/width ratios similar to glacially carved valleys (e.g. Gürbüz, 2010; Hempton and Dunne, 1984). Furthermore, the dimensions of the Mariana Pimentel Paleovalley do not correspond well with the Namibian paleovalleys (e.g. Martin, 1981) to which they are supposedly related. The Namibian paleovalleys, which contain glacial features, range in width from ~7–13 km as compared to the Mariana Pimentel Paleovalley that range from ~0.5–6.5 km wide.

6.6. Implications for the extent of glaciation in west-central Gondwana

A non-glacial interpretation of the paleovalleys and the lack of African-sourced zircons contradict the hypothesis that outlet glaciers flowed directly onto the RGS from the Windhoek Highlands (Namibia) through a series of glacially-carved fjords (Fig. 2D). Additionally, the lack of African provenance for sediments on the RGS, combined with previously described grooved surfaces on the western RGS showing ice flow towards the N-NW (i.e. Tomazelli and Soliani Júnior, 1982; Tomazelli and Soliani Júnior, 1997), do not support the hypothesis that large, unconfined lobes from Africa or Antarctica extended E to W across the RGS (Fig. 2B).

Importantly, this study does not negate the clear evidence for glaciation on the western RGS (e.g. Tomazelli and Soliani Júnior, 1982; Tomazelli and Soliani Júnior, 1997). Additionally, it does not contradict the hypothesis that outlet glaciers from Africa may have flowed through bedrock lows onto the eastern margin of the basin (e.g. Fallgatter and Paim, 2017). Rather, combined with ice flow directions from other studies (i.e. Amato, 2017; Tomazelli and Soliani Júnior, 1982; Tomazelli and Soliani Júnior, 1997), these results are in agreement with the hypothesis proposed by Crowell and Frakes (1975) that a separate, unconfined ice lobe extended N-NW out of Uruguay across the western RGS (Fig. 2C). This "Uruguayan Lobe" may have originated in

southern Africa, or it may have nucleated on the Rio de la Plata Craton (Uruguay and Argentina). Although an ice advance out of Uruguay may have predated the formation of the paleovalleys on the eastern half of the RGS, evidence for such an event is currently unsubstantiated.

The other possibility, that glaciation on the RGS existed as standalone, small ice caps or alpine glaciers (e.g. Santos et al., 1996) can also not be ruled out based on the evidence presented here (Fig. 2A). Regardless, it seems probable that glaciogenic sediments on the RGS have a separate provenance from the same lithostratigraphic unit (Taciba Fm.) on the eastern margin of the Paraná Basin. Along these same lines, the lack of an African detrital zircon signature within the paleovalleys makes it more difficult to link glaciation on the RGS (southernmost Paraná Basin) to extra-basinal deposits such as the Dwyka Gp. in the Greater Karoo Basin.

Separate ice centers on the southern and eastern margins of the Paraná Basin would have contained substantially less ice volume compared to a single, massive ice sheet. For comparison, a massive hypothetical ice sheet covering the entire RGS and the eastern margin of the basin, centered over western Africa, and measuring ~1,250,000 km² would be capable of producing ~4.6 m of global sealevel change. Two separate ice centers, of equal combined area, would produce ~3.9 m of global sea-level change (c.f. Crowley and Baum, 1991; Isbell et al., 2003). However, neither scenario would add significantly to some estimates of ~100–120 m of sea-level fluctuations during the Carboniferous and Permian (e.g. Chen et al., 2016; Rygel et al., 2008). If sea-level oscillations of such magnitudes occurred, contemporaneous with deposition in the Mariana Pimentel and Leão paleovalleys, the required ice center(s) must have existed elsewhere.

7. Conclusions

- (1) The facies assemblage from the Mariana Pimentel and Leão Paleovalley system does not support the previously hypothesized origin as a glacially-influenced depositional environment. The basal portion of the paleovalleys contains a transition from a non-glacial lacustrine or estuarine environment into a fluvial-dominated incised valley. The top portion of the paleovalley system fill consists of a restricted marine/estuarine facies association.
- (2) Detrital zircon geochronology results show a unimodal population of ages ranging from ~800–550 Ma. This is consistent with a local (non-African), Dom Feliciano Belt provenance for the sedimentary fill of the paleovalleys.
- (3) The facies assemblage, stratigraphy, and position of the paleovalleys within a Neoproterozoic shear zone suggest a tectonic control on the initial formation of the paleovalleys and the deposition of their fill. The Mariana Pimentel Paleovalley has many characteristics of a small pull-apart basin.
- (4) This study suggests that outlet glaciers from Namibia did not travel onto the RGS through a network of paleovalleys. It is also inconsistent with the hypothesis that a single, massive, unconfined ice sheet in Africa (or Antarctica) was responsible for deposition on both the eastern margin of the Paraná Basin and on the RGS (southern margin). The most likely source of glaciation on the RGS was a lobe, separate from the eastern margin of the Paraná Basin, which extended N-NW out of Uruguay onto the western RGS. Another possible explanation is that glaciation on the RGS was restricted to a small ice cap or alpine glaciers.
- (5) These findings are supportive of the general hypothesis that Carboniferous-Permian glaciation in west-central Gondwana was comprised of smaller, separate ice centers with less ice-volume than some previous estimates for this region.

Acknowledgments

The authors would like to thank the Companhia de Pesquia de Recursos Minerais (CPRM), the Universidade do Vale do Rio do Sinos (UNISINOS), and Dr. Ricardo Lopes for providing access to the cores utilized in this study. We would also like to thank Guilherme Roesler, João Ricetti, Dr. William Matsumara, Dr. Magda Huyskens, and Dr. Matthew Sanborn. This project was supported financially by grants from the U.S. National Science Foundation (OISE-1444181, OISE-1559231, and EAR-1729219 to JI; OISE-1444210 and EAR-1729882 to IPM), the UW-Milwaukee Research Growth Initiative (RGI), and Conselho Nacional de Desenvolvimento Científico e Tecnológico (CNPq, grants 461650/2014-2, 430096/2016-0, PQ 312747/2017-9). Other financial support was provided by the American Association of Petroleum Geologists (AAPG), the Geological Society of America (GSA), the Society for Sedimentary Geology (SEPM), the University of Wisconsin-Milwaukee Center for Latin American and Caribbean Studies (CLACS), the University of Wisconsin-Milwaukee Geosciences Department, the Wisconsin Geological Society, and Coordenação de Aperfeiçoamento de Pessoal de Nível Superior (CAPES).

Appendix A. Supplementary data

Supplementary data to this article can be found online at https://doi.org/10.1016/j.palaeo.2018.04.013.

References

- Amato, J.A., 2017. Using AMS to Help Interpret Glaciogenic Deposits of the Late Paleozoic Ice Age in the Paraná Basin, Brazil. University of Wisconsin-Milwaukee (Unpublished Masters Thesis, 162 pp.).
- Babinski, M., Chemale Jr., F., Van Schmus, W.R., Hartmann, L.A., Silva, da L.C., 1997. U–Pb and Sm–Nd geochronology of the Neoproterozoic granitic-gneissic Dom Feliciano Belt, southern Brazil. J. S. Am. Sci. 10, 263–274.
- Benn, D.I., Evans, D.J.A., 2010. Glaciers and Glaciation. Hodder Education, London, pp. 802.
- Bennett, M.R., Doyle, P., Mather, A.E., 1996. Dropstones: their origin and significance. Palaeogeogr. Palaeoclimatol. Palaeoecol. 121, 331–339.
- Buggisch, W., Wang, X., Alekseev, A.S., Joachimski, M.M., 2011. Carboniferous-Permian carbon isotope stratigraphy of successions from China (Yangtze platform), USA (Kansas) and Russia (Moscow Basin and Urals). Palaeogeogr. Palaeoclimatol. Palaeoecol. 301, 18–38.
- Bull, W.B., 1977. The alluvial-fan environment. Prog. Phys. Geogr. 1, 222-270.
- Cagliari, J., Philipp, R.P., Buso, V.V., Netto, R.G., Hillebrand, P.K., Lopes, R.D.C., Basei, M.A.S., Faccini, U.F., 2016. Age constraints of the glaciation in the Paraná Basin: evidence from new U-Pb dates. J. Geol. Soc. 173, 871–874.
- Canile, F.M., Babinski, M., Rocha-Campos, A.C., 2016. Evolution of the Carboniferous-Early Cretaceous units of the Paraná Basin from provenance studies based on U-Pb, Hf and O isotopes from detrital zircons. Gondwana Res. 40, 142–169.
- Carto, S., Eyles, N., 2012. Sedimentology of the Neoproterozoic (c. 580 Ma) Squantum 'Tillite', Boston Basin USA: mass flow deposition in a deep-water arc basin lacking direct glacial influence. Sediment. Geol. 269, 1–14.
- Chen, B., Joachimski, M.M., Shen, S., Lambert, L.L., Lai, X., Wang, X., Chen, J., Yuan, D., 2013. Permian ice volume and palaeoclimate history: oxygen isotope proxies revisited. Gondwana Res. 24, 77–89.
- Chen, B., Joachimski, M.M., Wang, X., Shen, S., Qi, Y., Qie, W., 2016. Ice volume and paleoclimate history of the late Paleozoic ice age from conodont apatite oxygen isotopes from Naqing (Guizhou, China). Palaeogeogr. Palaeoclimatol. Palaeoecol. 448, 151–161.
- Cordani, U.G., Sato, K., Teixeira, W., Tassianri, C.C.G., Basei, M.A.S., 2000. Crustal evolution of the South American Platform. In: Cordani, U.G., Milani, E.J., Thomaz Filho, A., Campos, D.A. (Eds.), Tecontic Evolution of South America. International Geological Congress 31, Rio de Janeiro, pp. 19–40.
- Corrêa da Silva, Z.C., 1978. Observações sobre o Grupo Tubarão no Rio Grande do Sul, com especial destaque á estratigrafia da Formação Itararé. Pesquisas—UFRGS 9, 27–44.
- Cowan, E.A., Powell, R.D., 1990. Suspended sediment transport and deposition of cyclically interlaminated sediment in a temperate glacial fjord, Alaska, U.S.A. In: Dowdeswell, J.A., Scourse, J.D. (Eds.), Glacimarine Environments: Processes and Sediments. 53. Geological Society Special Publication, pp. 75–89.
- Cowan, E.A., Seramur, K.C., Powell, R.D., Willems, B.A., Gulick, S.P.S., Jaeger, J.M., 2010. Fjords as temporary sediment traps: history of glacial erosion and deposition in Muir inlet, Glacier Bay National Park, southeastern Alaska. GSA Bull. 122, 1067–1080.
- Crookshanks, S., Gilbert, R., 2008. Continuous, diurnally fluctuating turbidity currents in Kluane Lake, Yukon territory. Can. J. Earth Sci. 45, 1123–1138.
- Crowell, J.C., 1999. Pre-Mesozoic ice ages: their bearing on understanding the climate system. Geol. Soc. Am. Mem. 192, 106 (Boulder).
- Crowell, J.C., Frakes, L.A., 1975. The late Paleozoic glaciation. In: Campbell, K.S.W. (Ed.), Gondwana Geology. Australian National University Press, Canberra, pp. 313–331.
- Crowley, T.J., Baum, S.K., 1991. Estimating Carboniferous sea-level fluctuations from Gondwana ice extent. Geology 19, 975–977.

- Dadson, S., Hovius, N., Pegg, S., Dade, W.B., Horng, M.J., Chen, H., 2005. Hyperpycnal river flows from an active mountain belt. J. Geophys. Res. 110, 4–16.
- de Wit, M.J., Stankiewicz, J., Reeves, C., 2008. Restoring Pan-African—Brasiliano connections: more Gondwana control, less trans-Atlantic corruption. In: Pankhurst, R.J., Trouw, R.A.J., Brito Neves, B.B., de Wit, M.J. (Eds.), West Gondwana: Pre-Cenezoic Correlations Across the South Atlantic Region. 294. Geological Society of London Special Publications, pp. 399–412.
- Delaney, P.I.V., 1964. Itararé outliers in Rio Grande do Sul, Brazil. Bol. Paranaen. Geogr. 10 (15). 161–173.
- Dionne, J.C., 1993. Sediment load of shore ice and ice rafting potential, Upper St. Lawrence Estuary, Quebec, Canada. J. Coast. Res. 9, 628–646.
- Doublet, S., Garcia, J.P., 2004. The significance of dropstones in tropical lacustrine setting, eastern Cameros Basin (Late Jurassic–Early Cretaceous, Spain). Sediment. Geol. 163, 293–309.
- Dowdeswell, J.A., Villinger, H., Whittington, R.J., Marienfeld, P., 1993. Iceberg scouring in Scoresby Sund and on the East Greenland continental shelf. Mar. Geol. 111, 37–53.
- Droser, M.L., Bottjer, D.J., 1986. A semiquantitative field classification of ichnofabric. J. Sediment. Petrol. 56, 558–559.
- Enos, P., 1977. Flow regimes in debris flow. Sedimentology 24, 133-142.
- Fallgatter, C., Paim, P.S.G., 2017. On the origin of the Itararé Group basal nonconformity and its implications for the late Paleozoic glaciation in the Paraná Basin, Brazil. Palaeogeogr. Palaeoclimatol. Palaeoecol. http://dx.doi.org/10.1016/j.palaeo.2017. 02.039. In Press.
- Farrell, K.M., Harris, W.B., Mallinson, D.J., Culver, S.J., Riggs, S.R., Pierson, J., Self-Trail, J.M., Lautier, J.C., 2012. Standardizing texture and facies codes for a process-based classification of clastic sediment and rock. J. Sediment. Res. 82, 364–378.
- Ferguson, L., 1970. "Armored snowballs" and the introduction of coarse terrigenous material into sea-ice. J. Sediment. Petrol. 40, 1057–1060.
- Fernandes, L.A.D., Koester, E., 1999. The Neoproterozoic Dorsal de Canguçú strike-slip shear zone: its nature and role in the tectonic evolution of southern Brazil. J. Afr. Earth Sci. 29, 3–24.
- Fielding, C.R., 1987. Coal depositional models for deltaic and alluvial plain sequences. Geology 15, 661–664.
- Fielding, C.R., Frank, T.D., Birgenheier, L.P., Rygel, M.C., Jones, A.T., Roberts, J., 2008a. Stratigraphic record and facies associations of the late Paleozoic ice age in eastern Australia (New South Wales and Queensland). In: Fielding, C.R., Frank, T.D., Isbell, J.L. (Eds.), Resolving the Late Paleozoic Ice Age in Time and Space. 441. Geological Society of America Special Publication, pp. 41–57.
- Fielding, C.R., Frank, T.D., Isbell, J.L., 2008b. The late Paleozoic ice age-A review of current understanding and synthesis of global climate patterns. In: Fielding, C.R., Frank, T.D., Isbell, J.L. (Eds.), Resolving the Late Paleozoic Ice Age in Time and Space. 441. Geological Society of America Special Publication, pp. 343–354.
- Foster, D.A., Goscombe, B.D., Newstead, B., Mapani, B., Mueller, P.A., Gregory, L.C., Muvangua, E., 2015. U-Pb age and Lu-Hf isotopic data of detrital zircons from the Congo and Kalahari before Gondwana. Gondwana Res. 28, 179–190.
- Frakes, L.A., Crowell, J.C., 1972. Late Paleozoic glacial geography between the Paraná Basin and the Andean Geosyncline. An. Acad. Bras. Cienc. 44, 139–145.
- França, A.B., Potter, P.E., 1991. Stratigraphy and reservoir potential of glacial deposits of the Itararé Group (Carboniferous-Permian), Paraná Basin, Brazil. AAPG Bull. 75, 62–85.
- Frank, T.D., Shultis, A.I., Fielding, C.R., 2015. Acme and demise of the late Paleozoic ice age: a view from the southeastern margin of Gondwana. Palaeogeogr. Palaeoclimatol. Palaeoecol. 418. 176–192.
- Garden, C.J., Craw, D., Waters, J.M., Smith, A., 2011. Rafting rocks reveal marine biological dispersal: a case study using clasts from beach-cast macroalgal holdfasts. Estuar. Coast. Shelf Sci. 95, 388–394.
- Gastal, M.C.P., Lafon, J.M., Hartmann, L.A., Koester, E., 2005. Sm–Nd isotopic compositions as a proxy for magmatic processes during the Neoproterozoic of the southern Brazilian shield. J. S. Am. Earth Sci. 18, 255–276.
- Gastaldo, R.A., DiMichele, W.A., Pfefferkorn, H.W., 1996. Out of the icehouse into the greenhouse; a late Paleozoic analog for modern global vegetational change. GSA Today 6, 1–7.
- Gesicki, A.L.D., Riccomini, C., Boggianic, P.C., Coimbra, A.M., 1998. The Aquidauana Formation (Paraná Basin) in the context of the late Paleozoic glaciation in western Gondwana. J. Afr. Earth Sci. 27, 81–82.
- Gesicki, A.L.D., Riccomini, C., Boggianic, P.C., 2002. Ice flow direction during late Paleozoic glaciation in western Paraná Basin, Brazil. J. S. Am. Earth Sci. 14, 933–939.
- Gilbert, R., 1990. Rafting in glacimarine environments. In: Dowdeswell, J.A., Scourse, J.D. (Eds.), Glacimarine Environments: Processes and Sediments. 53. Geological Society of London Special Publications, pp. 105–120.
- Girardclos, S., Schmidt, O.T., Sturm, M., Ariztegui, D., Pugin, A., Anselmetti, F.S., 2007. The 1996 AD delta collapse and large turbidite in Lake Brienz. Mar. Geol. 241, 137–154.
- Gray, D.R., Foster, D.A., Meert, J.G., Goscombe, B.D., Armstrong, R., Trouw, R.A.J., Passchier, C.W., 2008. A Damara orogeny perspective on the assembly of southwestern Gondwana. In: Pankhurst, R.J., Trouw, R.A.J., Brito Neves, B.B., De Wit, M.J. (Eds.), West Gondwana: Pre-Cenozoic Correlations Across the South Atlantic Region. 294. Geological Society of London Special Publications, pp. 257–278.
- Griffis, N.P., Mundil, R., Montañez, I.P., Isbell, J.L., Fedorchuk, N.D., Vesely, F.F., Iannuzzi, R., Yin, Q., 2018. A new stratigraphic framework built on U-Pb single zircon TIMS ages with implications for the timing of the penultimate icehouse (Paraná Basin, Brazil). GSA Bull (In Press).
- Guerra-Sommer, M., Cazzulo-Klepzig, M., Menegat, R., Mendonça, J.G., 2008a. U-Pb dating of tonstein layers from a coal succession of the southern Paraná Basin (Brazil): a new geochronological approach. Gondwana Res. 14, 474–482.
- Guerra-Sommer, M., Cazzulo-Klepzig, M., Menegat, R., Formoso, M.L.L., Basei, M.A.S.,

- Barboza, E.G., Simas, M.W., 2008b. Geochronological data from the Faxinal coal succession, southern Paraná Basin, Brazil: a preliminary approach combining radiometric U-Pb dating and palynostratigraphy. J. S. Am. Earth Sci. 25, 246–256.
- Guerra-Sommer, M., Cazzulo-Klepzig, M., Santos, J.O.S., Hartmann, L.A., Ketzer, J.M.M., Formoso, M.L.L., 2008c. Radiometric age determination of tonsteins and stratigraphic constraints for the lower Permian coal succession in southern Paraná Basin, Brazil. Int. J. Coal Geol. 74, 13–27.
- Gulbranson, E.L., Montañez, I.P., Schmitz, M.D., Limarino, C.O., Isbell, J.L., Marenssi, S.A., Crowley, J.L., 2010. High-precision U-Pb calibration of Carboniferous glaciation and climate history, Paganzo Group, NW Argentina. GSA Bull. 122, 1480–1498.
- Gürbüz, A., 2010. Geometric characteristics of pull-apart basins. Lithosphere 2, 199–206. Gustavson, T.C., 1991. Buried vertisols in lacustrine facies of the Pliocene Fort Hancock Formation, Hueco Bolson, West Texas and Chihuahua, Mexico. GSA Bull. 103,
- Guy-Ohlson, D., 1996. Chapter 7B. Prasinophycean algae. In: Jansonius, J., McGregor, D.C. (Eds.), Palynology: Principles and Applications. 1. American Association of Stratigraphic Palynologists Foundation, pp. 181–189.
- Hambrey, M.J., Glasser, N.F., 2003. Glacial sediments: processes, environments and facies. In: Middleton, G.V. (Ed.), Encyclopedia of Sediments and Sedimentary Rocks. Kluwer, Dordrecht, pp. 316–331.
- Hempton, M.R., Dunne, L.A., 1984. Sedimentation in pull-apart basins: active examples in eastern Turkey. J. Geol. 92, 513–530.
- Holz, M., 1999. Early Permian sequence stratigraphy and the palaeophysiographic evolution of the Paraná Basin in southernmost Brazil. J. Afr. Earth Sci. 29, 51–61.
- Holz, M., 2003. Sequence stratigraphy of a lagoonal estuarine system—an example from the lower Permian Rio Bonito Formation, Paraná Basin, Brazil. Sediment. Geol. 162, 305–331.
- Holz, M., Küchle, J., Philipp, R.P., Bischoff, A.P., Arima, N., 2006. Hierarchy of tectonic control on stratigraphic signatures: base-level changes during the Early Permian in the Paraná Basin, southernmost Brazil. J. S. Am. Earth Sci. 22, 185–204.
- Holz, M., Souza, P.A., Iannuzzi, R., 2008. Sequence stratigraphy and biostratigraphy of the Late Carboniferous to Early Permian glacial succession (Itararé subgroup) at the eastern-southeastern margin of the Paraná Basin, Brazil. In: Fielding, C.R., Frank, T., Isbell, J.L. (Eds.), Resolving the Late Paleozoic Ice Age in Time and Space. 441. Geological Society of America Special Paper, pp. 115–129.
- Holz, M., França, A.B., Souza, P.A., Iannuzzi, R., Rohn, R., 2010. A stratigraphic chart of the Late Carboniferous/Permian succession of the eastern border of the Paraná Basin, Brazil, South America. J. S. Am. Earth Sci. 29, 381–399.
- Horton, D.E., Poulsen, C.J., Pollard, D., 2010. Influence of high-latitude vegetation feedbacks on late Palaeozoic glacial cycles. Nat. Geosci. 3, 572–577.
- Iannuzzi, R., Pfefferkorn, H.W., 2002. A pre-glacial, warm-temperate floral belt in Gondwana (Late Visean, Early Carboniferous). PALAIOS 17, 571–590.
- Iannuzzi, R., Scherer, C.M.S., Souza, P.A., Holz, M., Caravaca, G., Adami-Rodrigues, K., Tybusch, G.P., Souza, J.M., Smaniotto, L.P., Fischer, T.V., Silveira, A.S., Lykawka, R., Boardman, D.R., Barboza, E.G., 2006. Afloramento Morro do Papaléo, Mariana Pimentel, R.S., Registro ímparda sucessão pós-glacial do Paleozóico da Bacia do Paraná. In: Winge, M., Schobbenhaus, C., Souza, C.R.G., Fernandes, A.C.S., Queiroz, E.T., Berbert-Born, M.L.C., Campos, D.A. (Eds.), Sítios Geológicos e Paleontológicos do Brasil. 2. pp. 1–13.
- Iannuzzi, R., Souza, P.A., Holz, M., 2010. Stratigraphic and paleofloristic record of the lower Permian postglacial succession in the southern Brazilian Paraná Basin. Geol. Soc. Am. Spec. Pap. 468, 113–132.
- Isbell, J.L., Miller, M.F., Wolfe, K.L., Lenaker, P.A., 2003. Timing of late Paleozoic glaciation in Gondwana: was glaciation responsible for the development of Northern Hemisphere cyclothems? Geol. Soc. Am. Spec. Pap. 370, 5–24.
- Isbell, J.L., Henry, L.C., Gulbranson, E.L., Limarino, C.O., Fraiser, M.L., Koch, Z.J., Ciccioli, P.L., Dineen, A.A., 2012. Glacial paradoxes during the late Paleozoic ice age: evaluating the equilibrium line altitude as a control on glaciation. Gondwana Res. 22, 1–19.
- Kempema, E.W., Ettema, R., 2011. Anchor ice rafting: observations from the Laramie River. River Res. Appl. 27, 1126–1135.
- Kempema, E.W., Reimnitz, E., Barnes, P.W., 2001. Anchor-ice formation and ice rafting in southwestern Lake Michigan, U.S.A. J. Sediment. Res. 71, 346–354.
- Kleiman, L.A., Japas, M.S., 2009. The Choiyoi volcanic province at 34°S–36°S (San Rafael, Mendoza, Argentina): implications for the late Paleozoic evolution of the southwestern margin of Gondwana. Tectonophysics 473, 283–299.
- Kwon, C.W., Jeong, J.O., Sohn, Y.K., 2011. Sedimentary records of rift to pull-apart tectonics in the Miocene Eoil Basin, SE Korea. Sediment. Geol. 236, 256–271.
- Leite, J.A.D., Hartmann, L.A., Fernandes, L.A.D., McNaughton, N.J., Soliani Jr., Ê., Koester, E., Santos, J.O.S., Vasconcellos, M.A.Z., 2000. Zircon U-Pb SHRIMP dating of gneissic basement of the Dom Feliciano Belt, southernmost Brazil. J. S. Am. Earth Sci. 13, 739-750.
- Lopes, R.d.C., 1995. Acabouço Aloestratigráfico para o Intervalo "Rio Bonito-Palermo" (Eopermiano da bacia do Paraná), entre Butiá e São Sepé, Rio Grande do Sul. Universidade do Vale do Rio do Sinos, São Leopoldo (Unpublished Masters Thesis, 254 pp.).
- López-Gamundí, O.R., 1997. Glacial-postglacial transition in the Late Paleozoic basins of southern South America. In: Martini, I.P. (Ed.), Late Glacial and Postglacial Environmental Changes: Quaternary, Carboniferous-Permian, and Proterozoic. Oxford University Press, Oxford, pp. 147–168.
- Mack, G.H., Rasmussen, K.A., 1984. Alluvial-fan sedimentation of the Cutler Formation (Permo-Pennsylvanian) near Gateway, Colorado. GSA Bull. 95, 109–116.
- Martin, H., 1981. The late Palaeozoic Dwyka Group of the South Kalahari Basin in Namibia and Botswana and the subglacial valleys of the Kaokoveld in Namibia. In: Hambrey, M.J., Harland, W.B. (Eds.), Earth's Pre-Pleistocene Glacial Record. Cambridge University Press, Cambridge, pp. 61–66.

- Martinsen, O.J., Ryseth, A., Helland-Hansen, W., Flesche, H., Torkildsen, G., Idil, S., 1999. Stratigraphic base level and fluvial architecture: Ericson sandstone (Campanian), Rock Springs Uplift, SW Wyoming, USA. Sedimentology 46, 235–259.
- Matos, S.L.F., Yamamoto, J.K., Riccomini, C., Hachiro, J., Tassinari, C.C.G., 2001.
 Absolute dating of Permian ash-fall in the Rio Bonito Formation, Paraná Basin, Brazil.
 Gondwana Res. 4, 421–426.
- Milani, E.J., Faccini, U.F., Scherer, C.M., Araújo, L.M., Cupertino, J.A., 1998. Sequences and Stratigraphic Hierarchy of the Paraná Basin (Ordovician to Cretaceous), Southern Brazil, Boletim IG USP. 29. pp. 125–173.
- Molnia, B.F., 1983. Subarctic glacial-marine sedimentation: a model. In: Molnia, B.F. (Ed.), Glacial-Marine Sedimentation. Plenum Press, New York, pp. 95–114.
- Montañez, I.P., Poulsen, C.J., 2013. The late Paleozoic ice age: an evolving paradigm. Annu. Rev. Earth Planet. Sci. 41, 1–28.
- Montañez, I., Soreghan, G.S., 2006. Earth's fickle climate; lessons learned from deep-time ice ages. Geotimes 51, 24–27.
- Montañez, I.P., Norris, R.D., Algeo, T., Chandler, M.A., Johnson, K.R., Kennedy, M.J., Kent, D.V., Kiehl, J.T., Kump, L.R., Ravelo, A.C., Turekian, K.K., Freeman, K.H., Feary, D.A., Rogers, N.D., Estep, J.T., Gibbs, C.R., Edkin, E.J., 2011. Understanding Earth's Deep Past; Lessons for Our Climate Future. National Academies Press, Washington, DC (194 pp.).
- Mori, A.L.O., de Souza, P.A., Marques, J.C., Lopes, R.d.C., 2012. A new U–Pb zircon age dating and palynological data from a Lower Permian section of the southernmost Paraná Basin, Brazil: Biochronostratigraphical and geochronological implications for Gondwanan correlations. Gondwana Res. 21, 654–669.
- Mugford, R.I., Dowdeswell, J.A., 2011. Modeling glacial meltwater plume dynamics and sedimentation in high-latitude fjords. J. Geophys. Res. 116, F01023.
- Nemec, W., Steel, R.J., 1984. Alluvial and coastal conglomerates: their significant features and some comments on gravelly mass-flow deposits. In: Koster, R.H., Steel, R.J. (Eds.), Sedimentology of Gravels and Conglomerates. 10. Canadian Society of Petroleum Geologists Memoirs, pp. 1–31.
- Ó Cofaigh, C., Dowdeswell, J.A., 2001. Laminated sediments in glacimarine environments: diagnostic criteria for their interpretation. Quat. Sci. Rev. 20, 1411–1436.
- Oliveira, C.H.E., Jelinek, A.R., Chemale Jr., F., Bernet, M., 2016. Evidence of post-Gondwana breakup in southern Brazilian shield: insights from apatite and zircon fission track thermochronology. Tectonophysics 666, 173–187.
- Ottensen, D., Dowdeswell, J.A., 2009. An inter-ice-stream glaciated margin: submarine landforms and a geomorphic model based on marine-geophysical data from Svalbard. GSA Bull. 121. 1647–1665.
- Oyhantçabal, P., Siegesmund, S., Wemmer, K., 2011. The Río de la Plata Craton: a review of units, boundaries, ages and isotopic signature. Int. J. Earth Sci. 100, 201–220.
- Paim, P.S.G., Piccoli, A.E.M., Sarturi, J.A.D., Munaro, P., Holz, M., Granitoff, W., 1983. Evolução paleogeográfica do Supergrupo Tubarãona área de Mariana Pimentel-Faxinal, Guaíba, RS. SBG, Simp. Sul-Brasileiro Geol. 1, 121–134.
- Passarelli, C.R., Basei, M.A.S., Wemmer, K., Siga Jr., O., Oyhantçabal, P., 2011. Major shear zones of southern Brazil and Uruguay: escape tectonics in the eastern border or Rio de La Plata and Paranapanema cratons during western Gondwana amalgamation. Int. J. Earth Sci. 100, 391–414.
- Philipp, R.P., Machado, R., 2005. The late Neoproterozoic granitoid magmatism of the Pelotas Batholith, southern Brazil. J. S. Am. Earth Sci. 19, 461–478.
- Posamentier, H.W., Martinsen, O.J., 2011. The character and genesis of submarine mass transport deposits; insights from outcrop and 3D seismic data. In: Shipp, R.G., Weimer, P., Posamentier, H.W. (Eds.), Mass-Transport Deposits in Deepwater Settings. 96. Society for Sedimentary Geology Special Publication, pp. 7–38.
- Postma, G., Nemec, W., Kleinspehn, K.L., 1988. Large floating clasts in turbidites: a mechanism for their emplacement. Sediment. Geol. 58, 47–61.
- Powell, R.D., 1990. Glacimarine processes at grounding-line fans and their growth to icecontact deltas. In: Dowdeswell, J.A., Scourse, J.D. (Eds.), Glacimarine Environments: Processes and Sediments. 53. Geological Society Special Publication, pp. 53–73.
- Powell, R.D., 2003. Subaquatic landsystems: fjords. In: Evans, D.A.J. (Ed.), Glacial Landsystems. Arnold, London, pp. 313–347.
- Ribeiro, N.V.B., Freitas, J.T., Souza, R., 1987. Correlação estratigráfica entre três bacias carboníferas do paleovale Leão/Mariana Pimentel. III Simpósio Sul Brasileiro de Geologia, Curitiba, Actas, pp. 335–350.
- Riccomini, C., Velázquez, V.F., 1999. Superfície estriada por geleira Neopaleozoica no Paraguai oriental. Rev. Basileira Geocienc. 29, 233–236.
- Ridgway, K.D., Decelles, P.G., 1993. Stream-dominated alluvial fan and lacustrine depositional systems in Cenozoic strike-slip basins, Denali fault system, Yukon Territory, Canada. Sedimentology 40, 645–666.
- Rocha-Campos, A.C., dos Santos, P.R., Canuto, J.R., 2008. Late Paleozoic glacial deposits of Brazil: Paraná Basin. In: Fielding, C.R., Frank, T.D., Isbell, J.L. (Eds.), Resolving the Late Paleozoic Ice Age in Time and Space. 441. Geological Society of America Special Papers, pp. 97–114.
- Rosa, E.L.M., Vesely, F.F., França, A.B., 2016. A review of the late Paleozoic ice-related erosional landforms in the Paraná Basin: origin and paleogeographical implications. Braz. J. Geol. 46, 147–166.
- Rygel, M.C., Fielding, C.R., Frank, T.D., Birgenheier, L.P., 2008. The magnitude of late Paleozoic glacioeustatic fluctuations: a synthesis. J. Sediment. Res. 500–511.
- Saalmann, K., Gerdes, A., Lahaye, Y., Hartmann, L.A., Remus, M.V.D., Läufer, A., 2011. Multiple accretion at the eastern margin of the Rio de la Plata craton: the prolonged Brasiliano orogeny in southernmost Brazil. Int. J. Earth Sci. 100, 355–378.
- Santos, P.R.D., Rocha-Campos, A.C., Canuto, J.R., 1996. Patterns of late Palaeozoic

- deglaciation in the Paraná Basin, Brazil. Palaeogeogr. Palaeoclimatol. Palaeoecol. 125. 165–184.
- Sarp, G., 2015. Tectonic controls on the North Anatolian Fault System (NAFS) on the geomorphic evolution of the alluvial fans and fan catchments in Erzincan pull-apart basin; Turkey. J. Asian Earth Sci. 98, 116–125.
- Schimmelmann, A., Lange, C.B., Schieber, J., Francus, P., Ojala, A.E.K., Zolitschka, B., 2016. Varves in marine sediments: a review. Earth Sci. Rev. 159, 215–246.
- Silva, da L.C., Hartmann, L.A., McNaughton, N.J., Fletcher, L.R., 1999. SHRIMP U/Pb zircon dating of Neoproterozoic granitic magmatism and collision in the Pelotas Batholith, southernmost Brazil. Int. Geol. Rev. 41, 531–551.
- Silveira, A.S., 2000. Estratigrafia de seqüências e evolução paleoambiental da sucessão Permiana (Sakmariano-Eokazaniano) da Bacia do Paraná, entre Rio Pardo e Mariana Pimentel (RS). Universidade do Vale do Rio do Sinos, São Leopoldo (Unpublished Masters Thesis, 140 p.).
- Simas, M.W., Guerra-Sommer, M., Cazzulo-Klepzig, M., Menegat, R., Santos, J.O.S., Ferreira, J.A.F., Degani-Schmidt, I., 2012. Geochronological correlation of the main coal interval in Brazilian Lower Permian: radiometric dating of tonstein and calibration of biostratigraphic framework. J. S. Am. Earth Sci. 39, 1–15.
- Smaniotto, L.P., Fischer, T.V., Souza, P.A., Iannuzzi, R., 2006. Palinologia do Morro do Papaléo, Mariana Pimentel (Permiano Inferior, Bacia do Paraná), Rio Grande do Sul, Brazil. Rev. Bras. Paleontol. 9, 311–322.
- Souza, P.A., 2006. Late Carboniferous palynostratigraphy of the Itararé Subgroup, northeastern Paraná Basin, Brazil. Rev. Palaeobot. Palynol. 138, 9–29.
- Syvitski, J.P.M., Burrell, D.C., Skei, J., 1987. Fjords: Processes and Products. Springer-Verlag, New York, pp. 379.
- Talling, P.J., 2014. On the triggers, resulting flow types and frequencies of subaqueous sediment density flows in different settings. Mar. Geol. 352, 155–182.
- Talling, P.J., Masson, D.G., Sumner, E.J., Malgesini, G., 2012. Subaqueous sediment density flows: depositional processes and deposit types. Sedimentology 59, 1937–2003.
- Tedesco, J., Cagliari, J., Coitinho, J.R., Lopes, R.C.L., Lavina, E.L.C., 2016. Late Paleozoic paleofjord in the southernmost Parana Basin (Brasil): geomorphology and sedimentary fill. Geomorphology 269, 203–214.
- Tomazelli, L.J., Soliani Júnior, E., 1982. Evidências de atividade glacial no Paleozóico Superior do Rio Grande do Sul, Brasil. 4. Anais II Congresso Brasileiro de Geologia, Salvador, pp. 1378–1389.
- Tomazelli, L.J., Soliani Júnior, E., 1997. Sedimentary facies and depositional environments related to Gondwana glaciation in Batovi and Suspiro Regions, Rio Grande do Sul, Brazil. J. S. Am. Earth Sci. 10, 295–303.
- Torsvik, T.H., Cocks, L.R.M., 2013. Gondwana from top to base in space and time. Gondwana Res. 24, 999–1030.
- Trzaskos, B., Vesely, F.F., Rostirolla, S.P., 2006. Recurrence of tectonic events overprint in the Carboniferous Vila Velha sandstones of the Itararé Group, Paraná Basin, South Brazil. Bol. Paranaen. Geociênc. 58, 89–104.
- van der Lingen, G.J., Pettinga, J.R., Balance, P.F., Reading, H.G., 1980. The Makara Basin: a Miocene slope-basin along the New Zealand sector of the Australian-Pacific obliquely convergent plate boundary. In: Sedimentation in Oblique-slip Mobile Zones. Blackwell Scientific Publications, Oxford, pp. 191–215.
- Veevers, J.J., Powell, C.McA., 1987. Late Paleozoic glacial episodes in Gondwanaland reflected in transgressive-regressive depositional sequences in Euramerica. Geol. Soc. Am. Bull. 98, 475–487.
- Vermeesch, P., 2012. On the visualization of detrital age distributions. Chem. Geol. 312-313, 190-194.
- Vermeesch, P., Resentini, A., Garzanti, E., 2016. An R package for statistical provenance analysis. Sediment. Geol. 336, 14–25.
- Vesely, F.F., Trzaskos, B., Kipper, F., Assine, M.L., Souza, P.A., 2015. Sedimentary record of a fluctuating ice margin from the Pennsylvanian of western Gondwana: Paraná Basin. southern Brazil. Sediment. Geol. 326. 45–63.
- Visser, J.N.J., 1987. The palaeogeography of part of southwestern Gondwana during the Permo-Carboniferous glacaiation. Palaeogeogr. Palaeoclimatol. Palaeoecol. 61, 205–219.
- Visser, J.N.J., 1993. A reconstruction of the late Palaeozoic ice sheet on southwestern Gondwana. In: Findlay, R.H., Unrug, R., Banks, M.R., Veevers, J.J. (Eds.), Gondwana 8 Assembly, Evolution and Dispersal. AA Balkema, Rotterdam, pp. 449–458.
- Visser, J.N.J., 1997. Deglaciation sequences in the Permo-Carboniferous Karoo and Kalahari basins of southern Africa: a tool in the analysis of cyclic glaciomarine basin fills. Sedimentology 44, 507–521.
- Waldron, J.W.F., 2004. Anatomy and evolution of a pull-apart basin, Stellarton, Nova Scotia. GSA Bull. 116, 109–127.
- Woodborne, M.W., Rogers, J., Jarman, N., 1989. The geological significance of kelprafted rock along the West Coast of South Africa. Geo-Mar. Lett. 9, 109–118.
- Ysufoğflu, H., 2013. An intramontane pull-apart basin in tectonic escape deformation: Elbistan Basin, eastern Taurides, Turkey. J. Geodyn. 65, 308–329.
- Zavala, C., Arcuri, M., 2016. Intrabasinal and extrabasinal turbidites: origin and distinctive characteristics. Sediment. Geol. 337, 36–54.
- Ziegler, A.M., Hulver, M.L., Rowley, D.B., 1997. Permian world topography and climate. In: Martini, I.P. (Ed.), Late Glacial and Post-glacial Environmental Changes-Quaternary, Carboniferous-Permian and Proterozoic. Oxford University Press, New York, pp. 111–146.
- Zolitschka, B., Francus, P., Ojala, A.E.K., Schimmelmann, A., 2015. Varves in lake sediments a review. Quat. Sci. Rev. 117, 1–41.